

**THE IMPACT OF DIFFERENT TROPOSPHERIC MODELS ON GPS
BASELINES IN GHANA**

KNUST
BY

EMMANUEL ATTA – OSEI, BSc. Geomatic Engineering (Hons)

A thesis submitted to the Department of Geomatic Engineering
Kwame Nkrumah University of Science and Technology

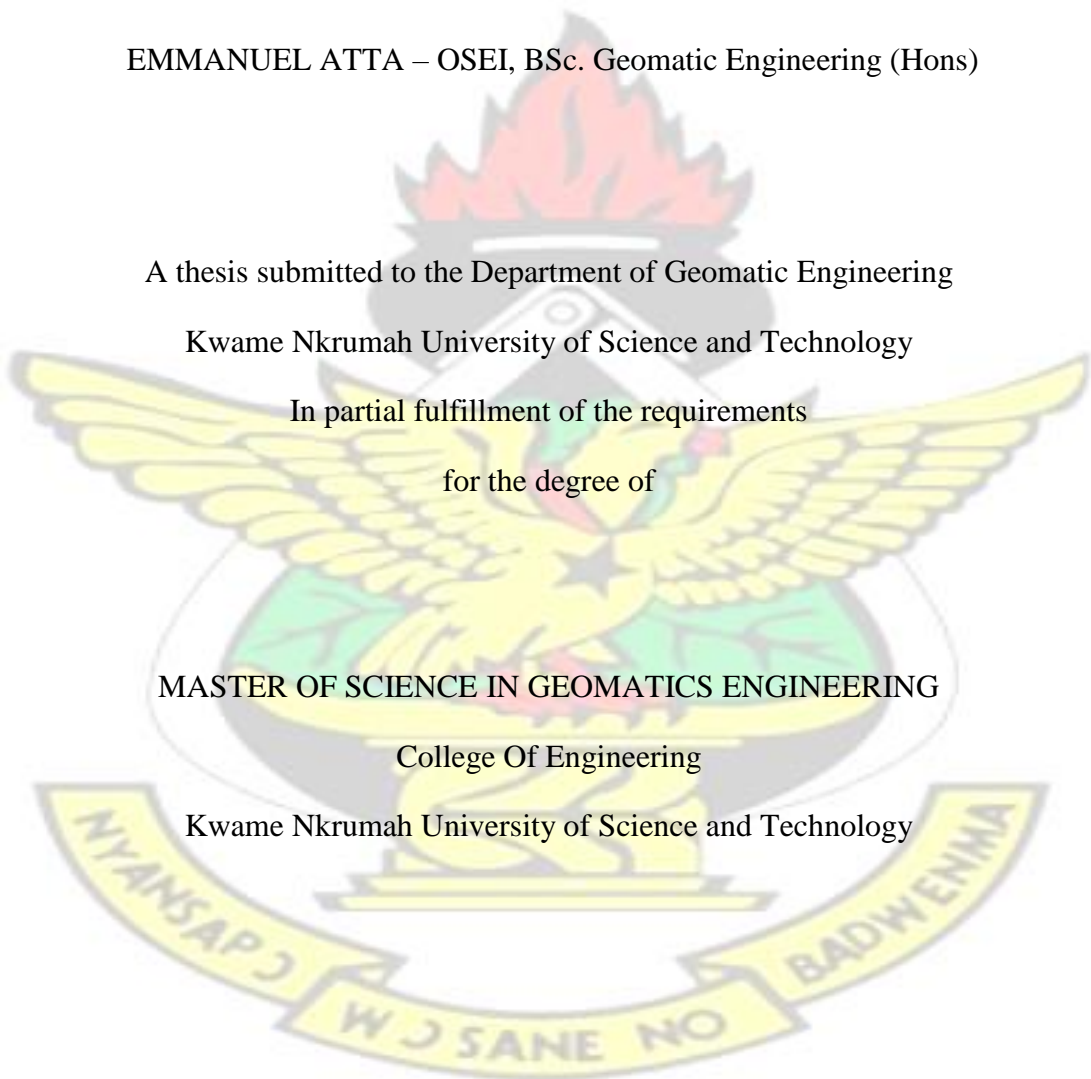
In partial fulfillment of the requirements

for the degree of

MASTER OF SCIENCE IN GEOMATICS ENGINEERING

College Of Engineering

Kwame Nkrumah University of Science and Technology



May, 2016

DECLARATION

I hereby declare that this submission is my own work towards the award of Master of Science degree and that, to the best of my knowledge, it contains neither material previously published by another person nor material which has been accepted for the award of any other degree of any university, except where due acknowledgement has been made in the text.

KNUST

Emmanuel Atta-Osei
(Student) Signature Date

Certified by:
Mr. Akwasi Afrifa Acheampong
(Supervisor) Signature Date

Certified by:
Prof. Dr. -Ing Collins Fosu
(Supervisor & Head of Department) Signature Date



ABSTRACT

The ionosphere and the troposphere are the two main layers in the atmosphere which delays GPS signals. Unlike the tropospheric bias, the ionospheric bias can be mitigated using dual frequency GPS receivers. Compensation for the tropospheric delays however requires a standard tropospheric model to be applied. Several tropospheric models are incorporated in commercial GPS processing software, including Trimble Geomatics Office (TGO), for correcting tropospheric delays. To investigate the impact of the different standard tropospheric models in TGO on GPS baselines so as to determine the best model for use by surveyors in Ghana, two simultaneous 24 hour observations were carried out at four selected COR stations in the Golden Triangle of Ghana. The RMS errors of the coordinates of the COR stations yielded by the five standard tropospheric models tested were **0.0287m** for Saastamoinen and Hopfield models, **0.0297m** for the Goad-Goodman model and **0.0317m** for both the Niell and Black models. The RMS errors from all the models passed the USACE criteria of 0.04m for long baselines beyond 100km. However, whenever a tropospheric model was ignored in the baseline processing, the RMS error was more than three times greater than the 0.04m accuracy limit. Surveyors must therefore avoid processing GPS baselines without tropospheric models. In conclusion, any of the five models evaluated in this study can perform well in the study area. Nevertheless, the choice of either the Hopfield or the Saastamoinen models is optimum for the processing of baselines in Ghana.



ACKNOWLEDGEMENT

I am most grateful to the Lord God Almighty for His sustenance and unlimited grace in Christ Jesus. The success of this research is because of His love divine, not mine.

I would like to express my deep gratitude to my supervisors; Prof. Dr.-Ing. Collins Fosu and Mr Akwasi Afrifa Acheampong for their unstinting support, guidance and scrutiny which I deem to be aboveboard.

My special thanks to my dearest brother and sponsor, Felix Atta-Okrah, who has been resolute in relieving me of every financial burden. Also to my mother, Grace Nsowa, the most important rung on my academic ladder. To my dad and my entire family.

Many thanks to Caroline Oye Otuei who provided, literally speaking, the daily inspiration I needed most. Carol, because your subtle pressure endured, my eventual pleasure has been assured. You are a wonderful counsellor, Stay blessed!

I am especially grateful to Brother Michael Oduro (BM), my first call after every incubus that came up with this research.

And finally, my abiding gratitude to my cherished colleagues at Ghana Bible College, brethren in the churches of Christ, and to those who desire to preach to the lost at all cost. God bless you all.

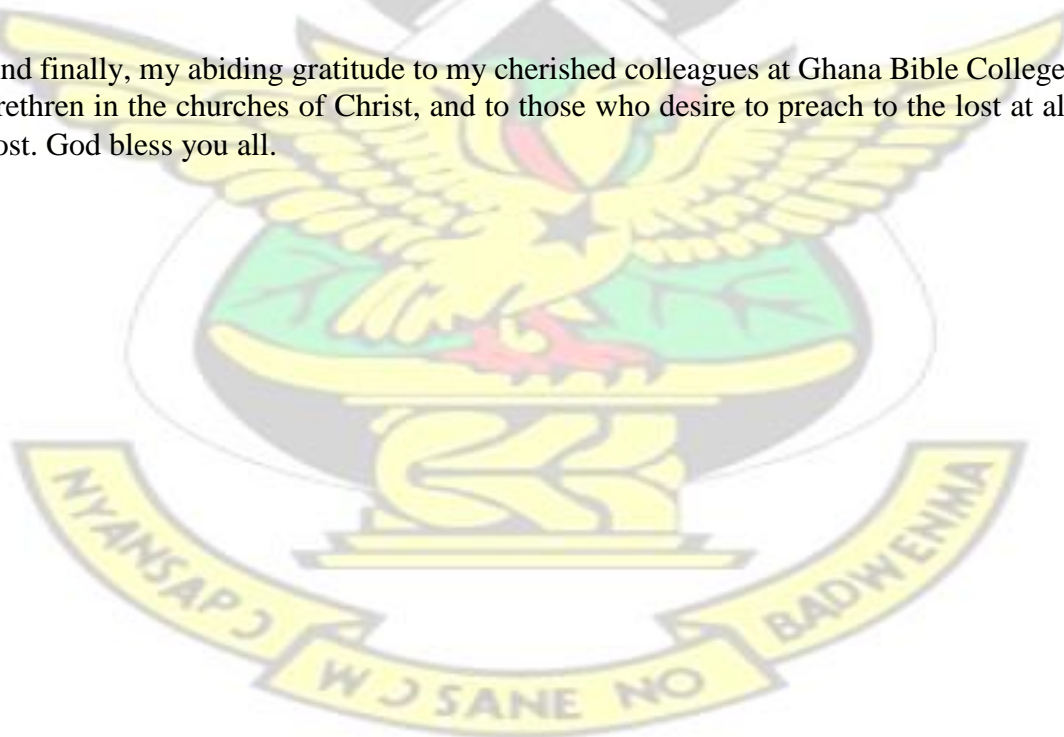


TABLE OF CONTENTS

DECLARATION	i
ABSTRACT	iii
ACKNOWLEDGEMENT	iv
TABLE OF CONTENTS	v
LIST OF FIGURES	viii
LIST OF TABLES	ix
CHAPTER ONE: INTRODUCTION.....	1
1.1 BACKGROUND	1
1.2 STATEMENT OF PROBLEM	3
1.3 AIM AND OBJECTIVES	4
1.4 STUDY AREA	5
1.5 STUDY OUTLINE	7
CHAPTER TWO: GNSS AND THE TROPOSPHERE	8
2.1 GLOBAL NAVIGATION SATELLITE SYSTEMS (GNSS)	8
2.1.1 THE GLOBAL POSITIONING SYSTEM (GPS)	9
2.1.2 GLONASS	11
2.1.3 GALILEO	11
2.1.4 COMPASS/BEIDOU	12
2.2 APPLICATIONS OF GNSS	13

2.3 GNSS ERROR SOURCES AND MITIGATION	14
2.3.1 SATELLITE-DEPENDENT ERRORS	15
2.3.1.1 EPHEMERIS ERRORS.....	15
2.3.1.2 CLOCK ERRORS	15
2.3.2 RECEIVER-DEPENDENT ERRORS	16
2.3.3 MULTIPATH	17
2.3.4 INTERFERENCE AND JAMMING	18
2.4 THE ATMOSPHERE AND ITS IMPACT ON GNSS SIGNALS	19
2.4.1 THE IONOSPHERIC IMPACT ON GNSS SIGNALS	20
2.4.2 THE TROPOSPHERE AND ITS IMPACT ON GNSS SIGNALS	23
2.5.1 TEMPERATURE AND PRESSURE VARIATIONS WITH ALTITUDE	27
2.6 TROPOSPHERIC MODELS AND MAPPING FUNCTIONS	27
2.6.1 THE SAASTAMOINEN MODEL	29
2.6.2 THE HOPFIELD MODEL	30
2.6.3 THE GOAD-GOODMAN MODEL.....	32
2.6.4 THE NIELL MODEL	33
2.6.5 THE BLACK MODEL	34
CHAPTER THREE: METHODOLOGY AND DATA PROCESSING	36
3.1 THE STUDY AREA	36
3.1.1 MONUMENTS	37
3.2 INSTRUMENTATION	38
3.2.1 RECEIVER	38

3.2.2 ANTENNA	39
3.3 DATA USED	40
3.4 DATA PRE-PROCESSING	40
3.4.1 ACCURACY LIMITS FOR DGPS BASELINES	41
3.4.2 USACE STANDARD FOR 100 KM:	41
3.4.3 SMD STANDARD FOR 100 KM:.....	41
3.5 DATA PROCESSING	42
3.6 TROPOSPHERIC EFFECTS ON BASELINES	43
3.7 NETWORK ADJUSTMENT	46
3.7.1 NETWORK PREADJUSTMENT DATA ANALYSIS	46
3.7.2 LOOP CLOSURE ANALYSIS	47
3.7.3 LEAST SQUARES ADJUSTMENT	50
3.7.3.1 OBSERVATION EQUATIONS	50
3.8 PROCESSING SOFTWARE	52
3.8.1 TRIMBLE GEOMATICS OFFICE (TGO)	53
CHAPTER 4: RESULTS AND ANALYSIS	54
4.1 RESULTS	54
4.2 ANALYSIS	56
CHAPTER 5: CONCLUSION AND RECOMMENDATION	60
5.1 CONCLUSION	60
5.2 RECOMMENDATIONS	62
REFERENCES	63

LIST OF FIGURES

Figure 1. 1 The study area on the National Map	6
Figure 1. 2 The study area with stations and baselines	6
Figure 2. 1 Segments of the GPS	10
Figure 2.2 GPS Signal Modernization	10
Figure 2.3 Illustrating the ephemeris error.....	15
Figure 2.4 Multipath ensuing from signal path deviation	17
Figure 2.5 Introduction to Interference	18
Figure 2.6 Layers of the Earth's atmosphere	20
Figure 2.7 The Earth's atmosphere and ionosphere	21
Figure 2.8: The Ionospheric regions	22
Figure 2.9: Layers in the atmosphere	24
Figure 2.10: The Dry and Wet Tropospheric Components	29
Figure 2.11: Geometry for the tropospheric path delay	32
Figure 3. 1 Map showing the study area with 100km coverage of permanent	37
Figure 3. 2 The three permanent Monuments of Ghana CORS Network	38
Figure 3. 3 GSR2600 receiver used in data collection	39
Figure 3. 4 A SOK702 antenna mounted on a tripod for data collection	39
Figure 3. 5 Data Processing Routine	45
Figure 3.6 GPS Observation Network	47
Figure 4. 1 The RMS trend with increasing observation time.	55
Figure 4. 2 RMS errors yielded by each Tropospheric Model	56
Figure 4. 3 Mean RMS error of various Tropospheric Models	56
Figure 4. 4 Deviation of other Models from the Optimum	57
Figure 4. 5 Juxtaposing RMS and Length of Baselines	58
Figure 4. 6 All models passed except for the NONE instance	59

LIST OF TABLES

Table 2.1 GLONASS constellation status.....	11
Table 2.2 Sections of the BeiDou Navigation Satellite System	13
Table 3.1 Data Quality Check Report	40
Table 3.2 Accuracy Limits for DGPS Baselines.....	41
Table 3.3 Precise Point Positions (PPP) of Stations	42
Table 3.4 The Solution Acceptance Criteria	43
Table 3.5 Resultant Loop Closure -Units (m)	49
Table 4.1 Baselines and their Designations	54
Table 4.2 Tropospheric Models and their Designations	54
Table 4.3 Baseline Processing Results- RMS Error per Tropospheric Model.....	55



CHAPTER ONE: INTRODUCTION

1.1 BACKGROUND

The indispensability of the Global Positioning System (GPS), or generally the Global Navigation Satellite System (GNSS), in modern geodetic techniques and other disciplines has necessitated investigations into the various errors affecting the system. Following the emission of signals by GNSS satellites, their propagation through the atmosphere to the receiver is delayed by the different refractive indices of the various atmospheric layers (Shrestha, 2003). Two main atmospheric subdivisions can be distinguished based on the way radio waves are propagated. These are: the ionosphere and the troposphere.

The ionosphere is the upper part of the atmosphere and is a region of charged particles with a large number of free electrons. It is a dispersive medium with a frequency-dependent propagation delay. The ionospheric bias can be mitigated using dual frequency GPS receivers. The troposphere however, is the lowest part of the electrically-neutral region of the atmosphere spanning from the earth's surface to about 8km at the poles and 16 km over the equator (Rizos, 1997). It is non-dispersive in nature and thus delays signals in a manner completely independent of their frequencies. The troposphere is an unstable layer, with significant atmospheric turbulence due to vertical convection currents, particularly within its boundary layer

i.e. the lowest 2 km of the troposphere (Kleijer, 2004).

Tropospheric delays can be separated into two main components (Hofmann-Wellenhof, et al, 2008):

- the hydrostatic delay and
- the wet delay

The hydrostatic delay is caused by the dry part of gases in the atmosphere, while the wet delay depends on the water vapor pressure. About 90% of the tropospheric delay is caused by the hydrostatic part (ibid). The hydrostatic delay is entirely dependent on the atmospheric weather characteristics found in the troposphere. Using measurements of surface temperature and pressure, the hydrostatic delays can be modeled and range corrections applied to obtain more accurate positioning results (Shrestha, 2003).

The wet tropospheric delay is hard to be completely mitigated and currently remains among the major residual error sources even in other space geodetic techniques like—DORIS (Doppler Orbitography and Radio-positioning Integrated by Satellite) and VLBI (Very Long Baseline Interferometry) (Opaluwa, et al., 2013).

Unless tropospheric delay effects are corrected, the height component of positions would be inaccurate especially in space-geodesy applications including sea-level

monitoring, post-glacial rebound measurements, earthquake-hazard mitigation, and crustal motion studies (Shrestha, 2003). These considerations are critical reasons for tropospheric delay modelling. It also gives credence to the incorporation of tropospheric models in most commercial GNSS processing software.

The availability of different tropospheric models is a further premise for probing into the impact of each of these models on baseline processing. This research seeks to assess how five selected tropospheric models affect the processing of GPS baselines in Ghana. Similar works done by other researchers prior to this one were all done outside Ghana and include the following: [Opaluwa, et al., 2013] who compared five standard dry tropospheric models in Minna, Nigeria. Also, a case study in Thailand assessed how different tropospheric models affected GPS baseline accuracy

(Chalermchon and Chalermwattanachai, 2005).

This project is unique for the:

1. **Use of Trimble Geomatics Office (TGO)**, a popular Commercial GNSS processing software, which is one of the various Trimble products used in over 100 countries around the world (Neal, 2008). Being a commercial software, TGO is easy to use and does not require so much time to understand. Expert training is also not necessary due to its simplicity (Blewitt, 1997).
2. **Reliance on the International Standard Atmosphere for relevant meteorological data.** This provides a precise alternative option (Hugentobler, et. al. , 2001) for Surveyors in Ghana who cannot afford expensive meteorological equipment for field use in projects which demand a higher accuracy.

It is anticipated that, findings from this pioneering research would be a vital contribution for further tropospheric studies in Ghana.

1.2 STATEMENT OF PROBLEM

Signal delays due to the impact of the troposphere remains a major challenge to GNSS positioning. Multiple models are available for the estimation of tropospheric delays. The level of refinement attainable with each of these models is however different. All the available standard tropospheric models were empirically derived from available radiosonde data, which were mostly obtained in the European and North American continents. Unfortunately, global constants are used in some standard tropospheric models. These disregard latitudinal and seasonal variations of parameters in the atmosphere (Roberts and Rizos, 2001).

Performance evaluation of different tropospheric delay models revealed that small discrepancies are present between the results of different models and that, all tested models performed significantly better at the mid-latitudes than at the Equator (Tuka & El-Mowafy, 2012). Also, high variations in water vapor content could exaggerate tropospheric effects derived from standard models (Mendes, 1999).

The impact of the tropospheric delay is even exacerbated by the use of single frequency receivers (Opaluwa, et al., 2013) which may be the only option for most GNSS users who may be unable to purchase dual frequency receivers due to the high cost. These GNSS users, especially surveyors, are further manacled by the prevalent limited research on how these various models affect baseline processing in our locality. It has therefore become expedient to study the impact of some of the prominent standard tropospheric models on the accuracy of GPS baselines in Ghana.

1.3 AIM AND OBJECTIVES

This research aims to recommend an optimum tropospheric model for Ghana by comparing the GPS positioning results derived from the use of five different standard tropospheric models, namely the Saastamoinen model, Hopfield model, GoadGoodman model, Niell model and Black model.

The following objectives are to assist in the attainment of the above aim:

- To estimate the amount of tropospheric delay yielded by each model for selected baselines by processing the observations using the Trimble Geomatics Office processing software.
- To assess the impact of baseline processing without any tropospheric model.

1.4 STUDY AREA

The project sites are Kumasi, Accra and Takoradi which constitute the golden triangle. The fourth station, Assin Fosu, is located within this triangle which according to Fosu, et. al. (2007) is of sides about 200km, covers three busiest highways and the whole of Ghana's railway line, plus over 85% of the coastline,

57.7% of the population and almost all the mines in Ghana.

Figure 1.1 shows the map of the study area as part of the entire map of Ghana. It is followed by Figure 1.2 which zooms into the study area and shows the stations in red, the station names in black (on a yellow background) and the baselines in green colours:



Figure 1. 1 The study area on the National Map



Figure 1. 2 The study area with stations and baselines

[NB. The figures above were extracted from google map. Not plotted to scale.]

1.5 STUDY OUTLINE

This thesis is organized into five chapters. This first chapter has clarified the need for the correction of tropospheric delays in high precision space geodetic applications.

Again, the statement of problem, study area and study objectives are also expounded.

Chapter Two contains a review of GNSS, their error sources, the structure of the troposphere and its effect on GPS signals. The chapter also presents the various types of tropospheric models and mapping functions.

Chapter Three explores the methodology used and describes the data acquisition and processing procedure. It describes the instruments used in the data collection and discusses their precision. It also presents all observations and data used as well as the processing software and the solutions recorded.

Chapter Four proceeds with the analysis and discussions of the results and findings. The performance of the various models are also evaluated and the optimal choice is made.

Chapter Five contains a summary of findings made, the conclusions drawn and proposes some recommendations for further research.

CHAPTER TWO: GNSS AND THE TROPOSPHERE

2.1 GLOBAL NAVIGATION SATELLITE SYSTEMS (GNSS)

GNSS is “a system of systems” (Turner, 2015). It encompasses the various satellite based systems which utilize radio signals to provide diverse world-wide services such as positioning, navigation, timing information and surveillance. The systems constituting the GNSS are listed below:

- GPS
- GLONASS
- GALILEO
- COMPASS/BEIDOU

These systems are supplemented by several space-based and ground based augmentation systems which are intended to boost regional services. Some are:

- The Wide Area Augmentation System (WAAS).
- The Russian System of Differential Correction and Monitoring (SDCM)
- The European Geostationary Navigation Overlay Service (EGNOS)
- GPS Aided Geo Augmented Navigation (GAGAN) / The Indian Regional Navigation Satellite System (IRNSS)
- The MASS – Multi-Functional Transport Satellite (MTSAT) Satellite Augmentation System.
- Quasi-Zenith Satellite System (QZSS)

2.1.1 THE GLOBAL POSITIONING SYSTEM (GPS)

The GPS is the result of a 1973 initiative by the US Department of Defense (DoD) which aimed to establish, develop, test, acquire, and deploy a spaceborne positioning system.

Wooden (1985) defined GPS as: “ an all-weather, space-based navigation system under development by the Department of Defense (DoD) to satisfy the requirements for the military forces to accurately determine their position, velocity, and time in a common reference system, anywhere on or near the earth on a continuous basis ” (Hofmann-Wellenhof, et al., 2008).

The Global Positioning System consists of the space, control and user segments.

- **The Space Segment** – It is composed of a nominal constellation of 24 satellites which transmit single-directional signals containing information on satellite position and time. As of May 18th, 2015, 31 satellites constituted the GPS constellation (Turner, 2015). The extra satellites beyond the nominal 24 are not part of the core constellation but are intended to ensure continual service in the event of servicing or decommissioning of any of the baseline satellites. The satellites orbit the Earth in a nominal orbital period of one-half of a sidereal day or 11 hours, 58 minutes (Kaplan & Hegarty, 2006).
- **The Control Segment** – It is constituted by worldwide stations for monitoring and controlling the space borne satellites. These stations also ensure that satellites are maintained in their proper orbits and occasionally command maneuvers as well as the adjustment of satellite clocks.

Figure 2.1 shows the three segments of GPS

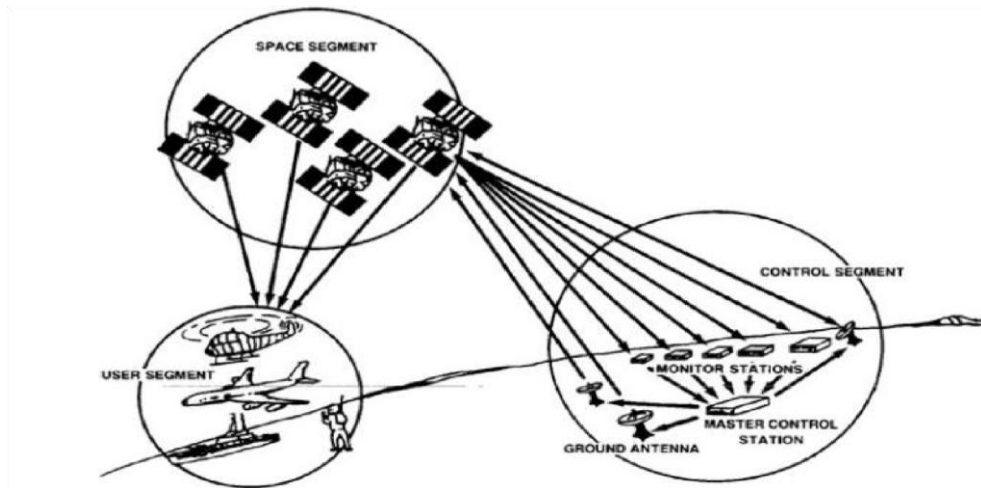


Figure 2. 1 Segments of the GPS

(Source: <http://www.gpc.se/press/wingtip7.gif>)

- **The User Segment** – It is made up of the GPS receiver equipment for the reception of signals and the calculation of the three dimensional position and time of users (GPS.gov, 2015).

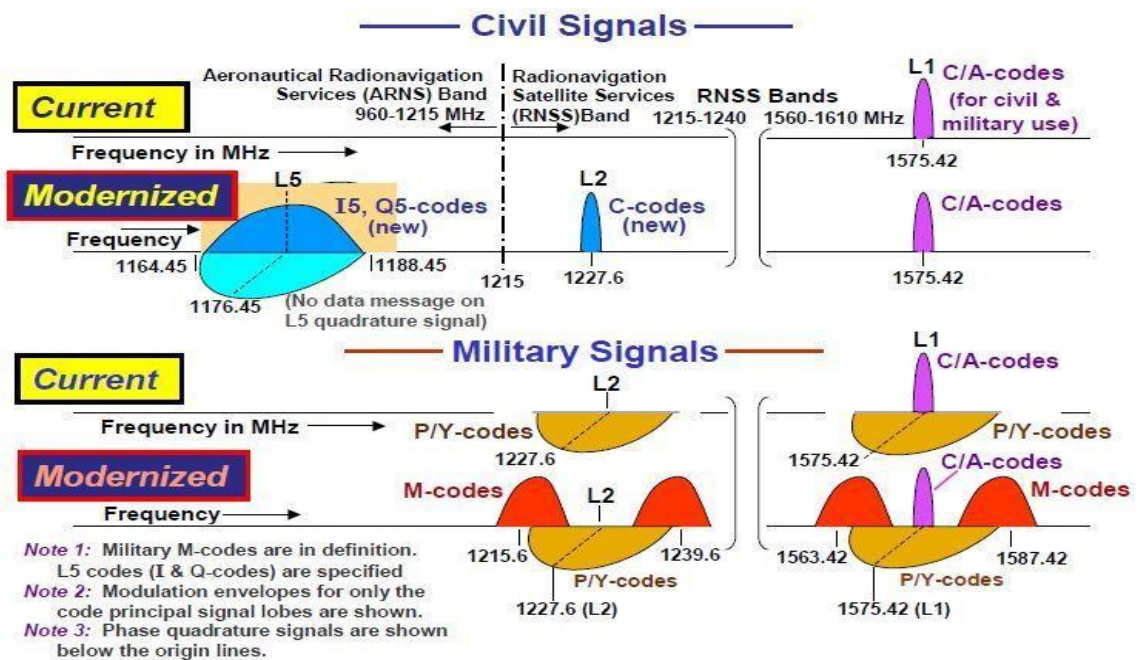


Figure 2.2 GPS Signal Modernization

(Source: McDonald, 2002)

Additional GPS information can be obtained from the official website: www.gps.gov

2.1.2 GLONASS

It is a Russian facility that provides a three-dimensional positioning, velocity and timing services for various multidisciplinary users in every part of the world, in any weather condition, and on a continuous basis (Hofmann-Wellenhof, et al., 2008).

GLONASS is comparable to the GPS with both systems having the same principles for the transmission of data and comparable techniques for positioning. GLONASS and GPS are not entirely compatible with each other but are generally interoperable (Guochang, 2007). GLONASS, however, unlike the GPS which uses the WGS84 datum and UTC time frame, GLONASS uses the PZ90 datum and UTC (Russia) time frame (Schofield & Breach, 2007).

Table 2. 1 GLONASS constellation status

Total Satellites in Constellation	28SC
Operational	24 SC
In commissioning phase	-
In maintenance	
Under check by the Satellite Prime Contractor	2 SC
Spares	-
In flight tests phase	2 SC

(Source: GLONASS, 2015)

Latest information can be accessed from the official website of GLONASS:

<https://glonass-iac.ru/en/>

2.1.3 GALILEO

Galileo is an European system envisioned to be controlled by civilians, unlike other military-originated systems, for the provision of very accurate and dependable positioning services at a global scale (ESA, 2015). It is interoperable with both GLONASS and GPS. Galileo is distinguished in its guaranteed availability of service (except in most challenging circumstances) and the assurance to notify users about any satellite failure, within seconds of such occurrences. This therefore makes it very appropriate for applications which are safety-critical (ibid).

The fully deployed Galileo system would consist of 30 satellites positioned in three circular Medium Earth Orbit (MEO) planes at 23,222 km altitude above the Earth, and

at an inclination of the orbital planes of 56 degrees to the equator. One satellite in each plane will be on stand-by to cater for any operational satellite failure (GSC, 2015).

Additional information about Galileo is available at: <http://www.gsa.europa.eu/>

2.1.4 COMPASS/BEIDOU

The BeiDou Navigation Satellite System (BDS) is a Chinese system. It formally began to provide services to the Asia-Pacific region in December 2012 and anticipates to provide global positioning, navigation and timing services around 2020 (CSNO, 2013) using two service modes:

- An Open Service and
- An Authorized Service.

The open service provides free of charge location, velocity and timing. It has a 10 meter and a 0.2 meter/second positioning and velocity accuracies respectively. It also has a timing accuracy of 10 nanoseconds. The authorized service will provide a more secure position, velocity, timing, and communications services in addition to a higher level of integrity (BDS, 2015).

BeiDou Navigation Satellite System is composed of three parts as illustrated in table 2.2

Table 2. 2 Sections of the BeiDou Navigation Satellite System

SECTION	DETAILS
The Space Section	<ul style="list-style-type: none"> • 5 geostationary orbit satellites and • 30 non-geostationary orbit satellites.
The Ground Section	<p>□ Consists of a number of stations including</p> <ul style="list-style-type: none"> ○ The Main Control Stations ○ The Injection Stations ○ The Monitoring Stations
The User Section	Includes terminators of Beidou System, and some compatible with other navigation satellite systems.

The official website of BeiDou is: <http://www.beidou.gov.cn>

2.2 APPLICATIONS OF GNSS

Global satellite navigation is an innovative facility which is impacting on several human undertakings. It is beneficial to individuals and nations in both simple and complex forms spanning from recreational to life dependent applications (Rasher, 2009). GNSS provides absolute and/or relative 3-D position, velocity and time data. This however, depends on the user's receiver type and the type of signals tracked.

The various applications offered by GNSS are of extreme miscellany and possess immense potential results. The technology is now incorporated in a variety of equipment for:

- Aerial, Terrestrial and Hydrographic Navigation and Monitoring with high precision. This entails measures to prevent collision, fleet monitoring, search and rescue activities etc.
- Aerial, Hydrographic and Terrestrial Surveying and Mapping- This involves the survey of geophysical resources, GIS data collection, etc. This application requires very high accuracies as well as special hardware and software that meet technical requirements.
- Military systems incorporate GNSS capabilities with much emphasis on dependability.
- Height measurements and deformation studies, meteorological applications, earthquake alert systems, disaster management, agricultural uses (precision farming) etc. (Rizos, 1997).
- Precise time synchronization for Communication networks, business and fiscal applications, power grids etc. Some wireless services are even inoperable in the absence of the GNSS facility.

2.3 GNSS ERROR SOURCES AND MITIGATION

The conspicuously important role played by the GNSS facility cannot be underestimated in geodetic, navigation, survey and several other sensitive disciplines. However, the accuracy, reliability and availability of the GNSS facility are also plagued by several errors or biases which are examined in the following subsections.

2.3.1 SATELLITE-DEPENDENT ERRORS

2.3.1.1 EPHEMERIS ERRORS

Ephemeris errors are differences between true satellite position and position computed using GNSS navigation message. At the various GNSS monitor stations (under the control segment), all satellites in orbit are tracked. This generates the ephemeris information of the various satellites.

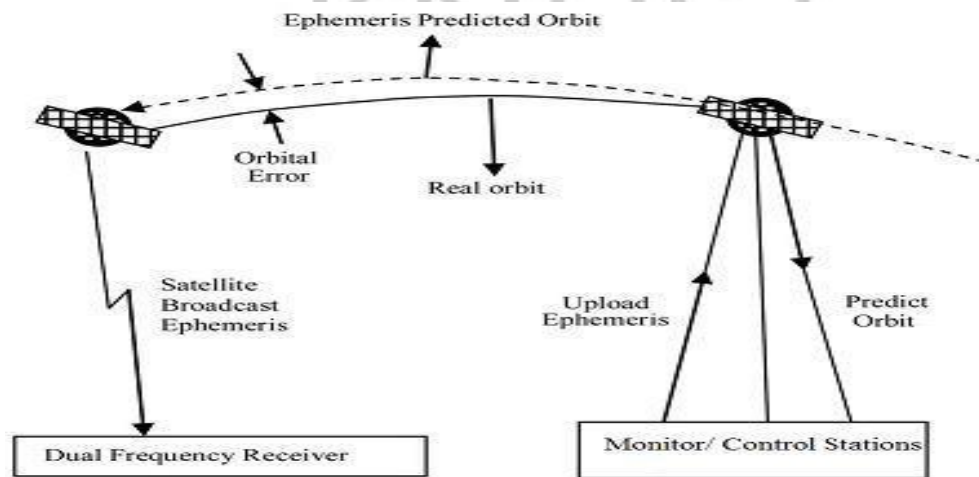


Figure 2.3 Illustrating the ephemeris error

Source: (Bidikar, et. al. , 2014)

Once this information is generated, it is followed by the computation of estimated ephemerides for the various satellites. The results (corrections) are uplinked so as to be rebroadcasted to the user. Such results proceed from a curve fit predicting the precise locations of each satellite during the moment of upload.

2.3.1.2 CLOCK ERRORS

GPS satellites have inbuilt atomic clocks for controlling all operations pertaining to time. A significant operation involves the generation of broadcast signals. In spite of its high stability, these onboard atomic clocks degrade with time due to the imperfect synchronization of the satellite oscillators to true time. This results in the satellite clock error which equally affects all users making concurrent observations to that same satellite (ibid). There is the need to correct this error in the context of high precision navigation applications.

The Master Control Station (MCS) computes the correction parameters based on a prediction curve-fit. These are then rebroadcasted to users in the navigation message. The resulting disparity between the MCS predictions and the actual satellite clock errors are known as residual clock errors. Whenever control segment uploads

corrections to satellites, the residual clock errors tend to be minimal but gradually degrades until the next upload (Conley, et al., 2006).

After adequately modelling the broadcast coefficients, the resulting satellite clock error is typically around 10 ns (Hugentober, et. al., 2001). A positional error of about 1-5 m and 0-1.5m may be introduced by ephemeris data and clock drift disparities respectively. (Heather and Christine, 2011).

2.3.2 RECEIVER-DEPENDENT ERRORS

GNSS receivers have inbuilt quartz crystal oscillators which are of low quality and stability in comparison to their atomic equivalents incorporated in satellites. This explains why the receiver clock errors cause inaccuracy in distance measurements and are generally higher than the satellite clock errors (Zheng, 2006). The receiver clocks have arbitrary origins which are required to be fixed to a well-established time scale. The disparity in receiver clock time and the GNSS time is referred to as the receiver clock error. This error equally affects every satellite tracked simultaneously by the same receiver (Acheampong, 2008).

2.3.3 MULTIPATH

When a GPS receiver receives signals reflected from surrounding objects plus the signals arriving from the satellite, multipath error is introduced (Sahmoudi and Landry, 2008). Hence, signals arrive at the receiver from multiple paths instead of the preferred direct path of the Line of Sight (LOS) signal. The magnitude of multipath errors depends considerably on the surroundings of the receiver (whether or not there are obstructing structures), the elevation angles, how the receiver processes signals, the type of signals and the antenna gain patterns (Conley, et al., 2006).

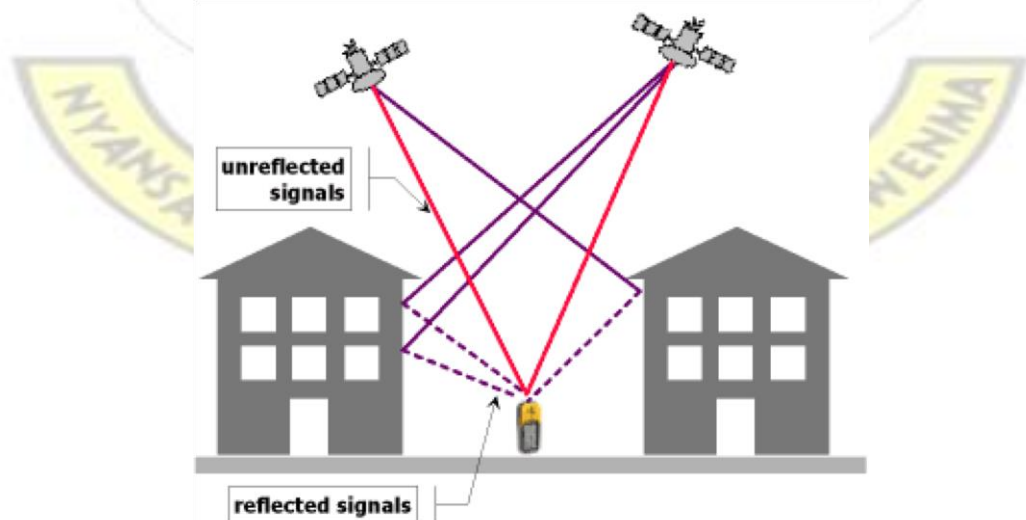


Figure 2.4 Multipath ensuing from signal path deviation

(Source: Kumar, 2014)

The following techniques, according to (Yedukondalu, et. al. , 2011), could be adopted to mitigate the effect of multipath:

- Placing antenna in locations with lower multipath impact. It is however a challenge to be assured of a site’s multipath effect before antenna installation.
- Hardware manufacturers could also reconsider the design of the antennae, the usage of microwave-absorbing materials etc.
- Other approaches related to software could be adopted. An instance is the development of algorithms which could reduce latent errors such as multipath.

2.3.4 INTERFERENCE AND JAMMING

Signals received by GNSS receivers from Radio Systems other than the desired source are known as interferences. They are mostly indeliberate as in the case of excess emissions from other authorized Radio Frequency systems. In the case where an interference proceeds from a deliberate action, it is designated as **jamming** (Kaplan and Hegarty, 2006). Figure 2.5 introduces the various categories of signal interference.

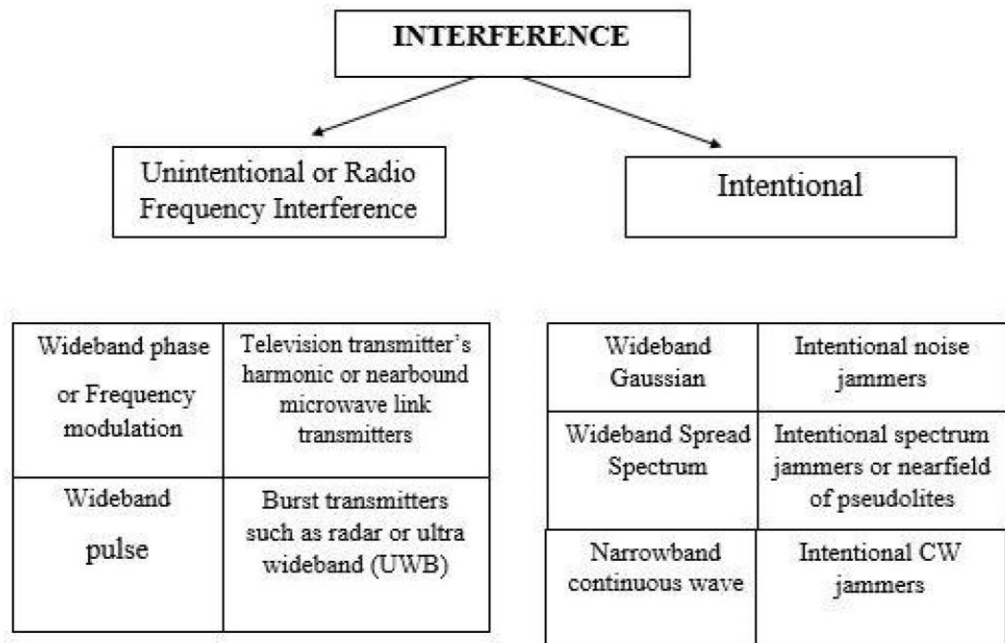


Figure 2.5 Introduction to Interference

(Source: Shytermeja, 2013)

The interference can significantly deteriorate the accuracy, integrity and availability of GNSS signal performances. The following two main techniques adapted from (Shytermeja, 2013) could be adopted to mitigate the challenge interference/jammers:

- Pre – Correlation Techniques: This includes- Amplitude Domain Processing, Dual Polarization Antenna, Spatial Filters, Space Time Filters etc.
- Post-Correlation Techniques such as Adaptive Loop Bandwidth, Data Wiping, Open Loop Carrier Tracking, Vector loops etc.

2.4 THE ATMOSPHERE AND ITS IMPACT ON GNSS SIGNALS

The atmosphere can be grouped into diverse layers based on their observable properties and how they influence electromagnetic waves. Considering the electromagnetic structure, two main divisions of the atmosphere can be made. These are the:

- Neutral atmosphere and
- Ionosphere.

The neutral section of the atmosphere can be further reclassified into the troposphere and stratosphere. The troposphere has however become a collective name for the neutral atmosphere. Consequently, the neutral atmospheric delay is also known, in

GNSS terminology, as “tropospheric delay” (Hofmann-Wellenhof, et. al., 2008). In

Figure 2.6, the various layers are illustrated.

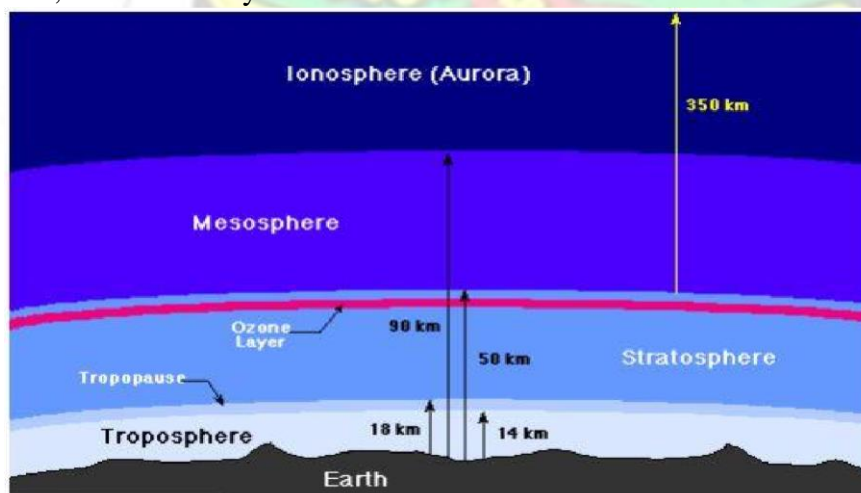


Figure 2.6 Layers of the Earth’s atmosphere

(Source: El-Arini, 2008)

Signals from GNSS satellites travel through the various atmospheric layers during their propagation from the satellites to their reception by the receivers. During the propagation of the signals through the neutral atmospheric layers, they are refracted by the various layers. These lead to **bending** of the paths of the signals causing delays. The impact is manifested in a longer distance between the satellite and receiver based on the signals arriving at the receiver end. This becomes evident when compared to the geometrical path of the same signal through a vacuum (Jensen, 2000).

KNUST

2.4.1 THE IONOSPHERIC IMPACT ON GNSS SIGNALS

The ionosphere lies from about 75 km to 1000 km range above the Earth. It has three main parts which are designated as the **D, E, and F regions**. The upper region (ie. the F) has maximum electron content. This region is ionized by solar radiation (in the daytime) and cosmic rays (at night). In comparison to the daytime, the D-region almost disappears in nocturnal sessions whilst the E-region also wanes (Stanford-Solar-Center, 2015).

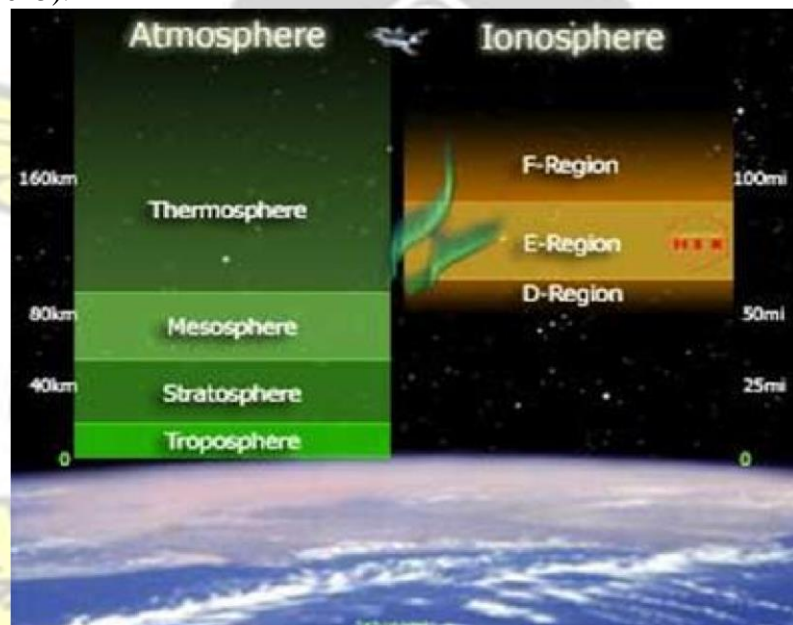


Figure 2.7 The Earth's atmosphere and ionosphere (ibid)

The ionosphere affects the GNSS signals in two main ways:

- **Refraction** - The effect of refraction on the propagated signals is as a result of the variation in electron content in the various ionospheric layers. This ensues in range measurement errors.
- **Diffraction** – This effect is as a result of plasma density anomalies. It leads to ionospheric scintillation and swift phase variations in the propagated signals.

The ionosphere is an electrically charged layer with notable characteristics of particles which are unrestrained, neutral, charged and diversified according to the particular time of day. In modelling the ionospheric refraction, it is expressed as a function of the electron density represented by the total electron content (TEC) (Hofmann-Wellenhof, et. al., 2008). The TEC is obtained by integrating the electron density along the satellite to receiver slant path. The unit for measuring TEC is electrons m^{-2} or TEC units (TEC_U) (Arbesser-Rastburg, 2002). The TEC varies with geomagnetic latitude, time, season, solar cycle etc. It is thus very difficult to model.

The ionosphere as shown in Figure 2.8 is categorized into 3 regions:

- **The Polar Region:** has the most unsteady TEC which is overly dependent on geomagnetic activities.
- **The Mid-Latitude Region:** has the least gradient of TEC and is by far the most steady.
- **The Equatorial Region:** has both the peak gradients and values of TEC.

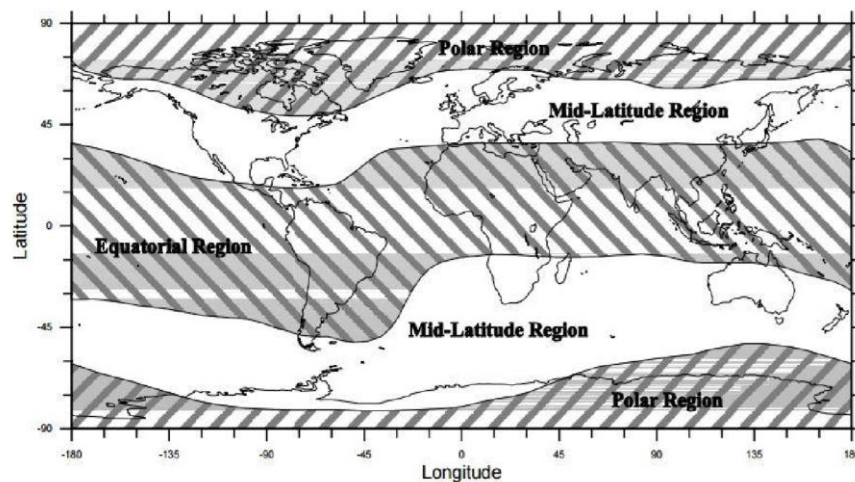


Figure 2.8: The Ionospheric regions

(Source: Warnant, 2002).

When crossing the ionosphere, both code and carrier signals are refracted, causing path lengthening and path shortening respectively. The delay of signals propagated through the ionosphere depends on frequency as a result of the dispersive nature of the ionospheric medium (Arbesser-Rastburg, 2002). Dual frequency GNSS receivers can therefore be used to obtain “ionosphere-free” solutions by using signals at two different frequencies.

In order to correct the ionospheric error, the following methods could also be utilized:

- Klobuchar model- It uses eight coefficients to represent the global ionosphere. When used by receiver based algorithms, the Klobuchar model can correct signal pseudoranges in real time.
- International Reference Ionosphere (IRI) model – it gives a comprehensive 3D electron density report on a global scale based on the assumption of the date, time and solar output.

2.4.2 THE TROPOSPHERE AND ITS IMPACT ON GNSS SIGNALS

The troposphere refers to the lowest atmospheric layer. It ranges from the earth's surface to **8km** at the pole, and to around **17km** at the equator. The troposphere is often construed in the GNSS community to include both the tropopause and the stratosphere. The troposphere therefore, in its more inclusive definition could reach up to about 50 km from the surface of the earth (Shrestha, 2003). This definition of the troposphere is used in this research.

The troposphere holds the major section of the total mass of the atmosphere (about 75%) with a primary composition of nitrogen (**78%**), oxygen (**20.9%**) and argon (**0.9%**) (ROB, 2012). As the lowest layer of the atmosphere, the troposphere is the host of rain, hail, snow etc. and other weather-related occurrences like clouds, weather fronts, thunderstorms etc. (ibid). The troposphere is a refractive medium and has a great impact on GNSS and other radio signals. It is non-dispersive for 30 GHz or less frequencies. The refractive index of the troposphere is dependent on the temperature, pressure, and partial water vapor pressure of the locality (HofmannWellenhof, et. al., 2008).

Tropospheric delays are classified into two main components (*ibid*):

- The hydrostatic delay and
- The wet delay



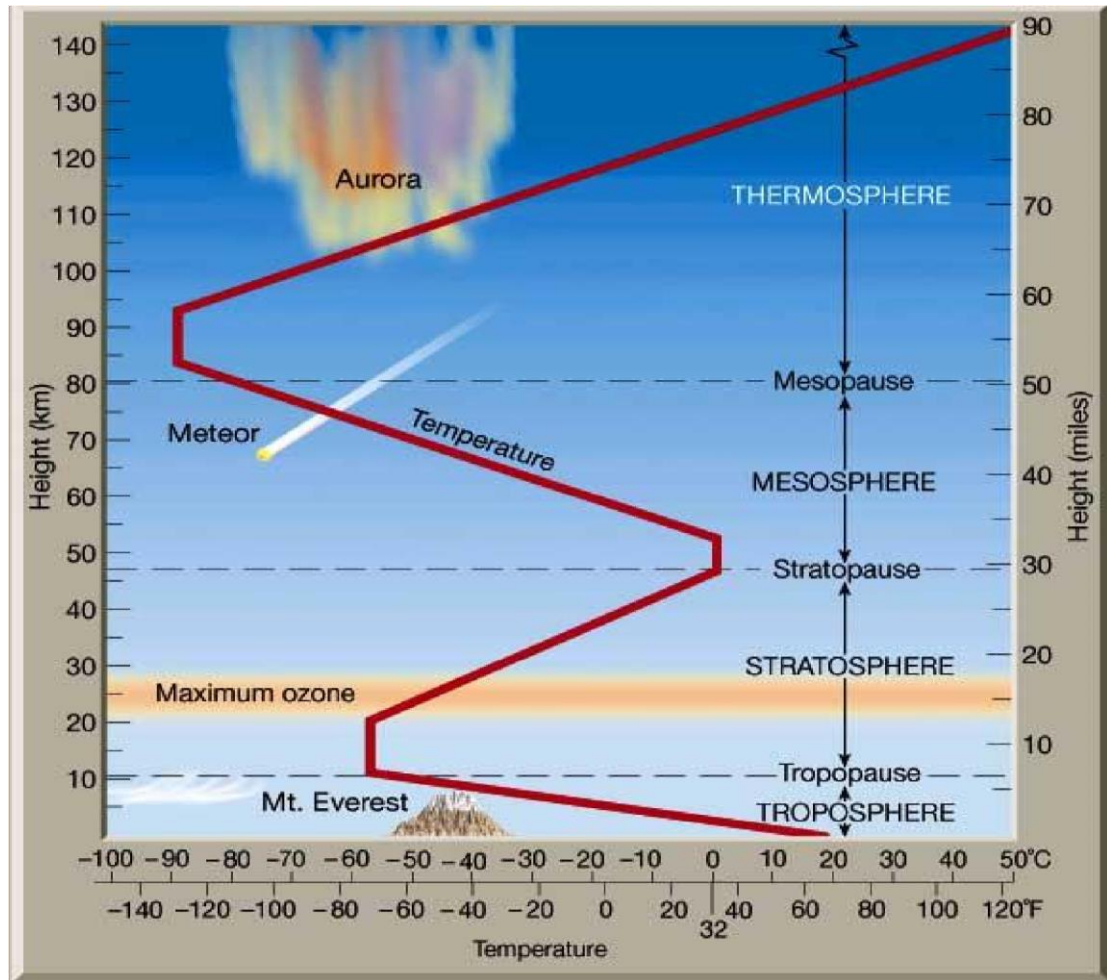


Figure 2.9: Layers in the atmosphere

(Source: Thinglink, 2016)

The hydrostatic delay is caused by the dry part of atmospheric gases, whereas the wet delay depends on the water vapor pressure. The hydrostatic part constitutes about 90% of the entire tropospheric delay (Hofmann-Wellenhof, et. al , 2008). The hydrostatic delay is completely dependent on the troposphere's meteorological conditions. It has a smooth, slowly time-varying characteristic and is often in hydrostatic equilibrium enabling the application of the ideal gas law (Opaluwa, et al., 2013).

Modelling of hydrostatic delays can be made by measuring surface temperature and pressure after which range corrections may be applied for very accurate positioning results (Shrestha, 2003). Alternatively, the model of a standard atmosphere may be used for a precise determination of hydrostatic delays (Hugentober, et. al, 2001). Further study on standard atmosphere is presented in Section 2.5 of this research.

The wet component, unlike the hydrostatic delay, is difficult to model precisely with surface measurements since it depends on liquid water and water vapor which are irregularly dispersed across the troposphere. Only about 10% of the total tropospheric delay is contributed by the wet component (Janes, et. al. , 1991). However, due to its

unpredictability, the wet component remains a latent factor inhibiting the determination of an absolute remediation of the total tropospheric delays. The situation is the same even in other techniques in space geodesy.

Examples are DORIS (Doppler Orbitography and Radio-positioning Integrated by Satellite) and VLBI (Very Long Baseline Interferometry). Wet delays can be recovered as the difference which remains after the hydrostatic delay has been taken from the total delay measured.

In measuring tropospheric delays, zenith signal delays are mapped to the various GPS satellites in view at a given receiver site using mapping functions such as Neill, Herring and Ifadis. Signal delays along the line of sight between individual satellites and the receiver are referred to as slant delays.

In the next chapter, some leading tropospheric models and mapping functions are examined in detail.

2.5 THE STANDARD ATMOSPHERE

The atmosphere of the earth is a constantly fluctuating system, always in a state of instability. The pressure and temperature of the atmosphere depend on altitude, location (longitude and latitude), and time of day, season, and even solar sunspot activity. The hypothetical standard atmospheric model approximates the multiple variations in the realistic atmosphere to a common reference.

The Standard Atmosphere is an artificial replica of the real atmosphere and is obtained as a mathematical abstraction of parameters from the real atmosphere. It is assumed to be the mean of average conditions of temperature, pressure, density and other properties as functions of altitude. Such values are obtained from experimental balloon and sounding-rocket measurements integrated with a mathematical model of the atmosphere (Yang, 2006). The standard atmosphere assumes its air to be absolutely still and without dust, moisture, and water vapour (i.e. without winds or turbulence) with respect to the Earth (Talay, 1975).

In 1952, the International Standard Atmosphere (ISA) was introduced by the International Civil Aviation Organisation (ICAO) after resolving the slight differences between the earliest models of the 1920's. The ISA specifies the following conditions at mean sea level (MSL) according to Cavcar (2014).

Pressure	$p(0) = 101325 \text{ N/m}^2 = 1013 \text{ hPa}$
Density	$\rho(0) = 1.225 \text{ kg/m}^3$
Temperature	$T(0) = 288.15 \text{ }^\circ\text{K} (15 \text{ }^\circ\text{C})$

Speed of Sound $a(o) = 340.294 \text{ m/sec}$

Acceleration due to gravity $g(o) = 9.80665 \text{ m/sec}^2$

2.5.1 TEMPERATURE AND PRESSURE VARIATIONS WITH ALTITUDE

Temperature is a function of altitude and varies at a constant rate known as the lapse rate. In the troposphere, the lapse rate is $-3.56616 \text{ degR}/1000\text{ft}$. It is only in the stratosphere that temperature remains constant even with change in altitude (Cavcar, 2014). The ISA parameters are calculated for a range of altitudes from sea level upward. The ISA considers the air to be a perfect gas and therefore calculates the various variations based on the following equations:

- Temperature variation

$$T = T_o - 6.5 \frac{h \text{ (m)}}{1000} \dots\dots\dots(1)$$

- The hydrostatic equation for a column of air: $dp = -\rho g \cdot dh \dots\dots\dots(2)$

- The equation of state for the perfect gas: $p = \rho R T \dots\dots\dots(3)$

Where:

h = altitude, m or ft
 p = pressure, N/m^2 or hPa

R = real gas constant for air, $287.04 \text{ m}^2/\text{°Ksec}^2$

T = temperature, °K or °C
 ρ = density, kg/m^3

2.6 TROPOSPHERIC MODELS AND MAPPING FUNCTIONS

It has been determined that, the tropospheric delay is directly proportional to the refractive index. It is given by (Hofmann-Wellenhof, et. al., 2008) as:

$$D^{\text{trop}} = \int (n - 1) ds \dots\dots\dots(4)$$

This can be expressed in terms of refractivity as:

$$D^{\text{trop}} = 10^6 \int N^{\text{trop}} ds \dots\dots\dots(5)$$

Comparing equations (4) and (5),

$$N = 10^6 (n - 1)$$

$$\text{trop} = 10^{-6} (n - 1) \dots\dots\dots(6)$$

Where N^{trop} = tropospheric refractivity and

n = refractive index

The impact of the troposphere on GNSS signals has already been examined in Section 2.8.5.2 where it has been established that, unlike ionospheric effects, tropospheric refraction cannot be eliminated by dual-frequency methods. Hence, the only option for the mitigation of tropospheric effect is to use models and/or to estimate from observational data (Subirana, et. al., 2011).

There are several tropospheric models in existence for the estimation of tropospheric delays. The typical differences between these models often pertain to the assumptions made on the vertical profiles and mappings (ibid). Some of the models are Geodetic-Oriented and others are Navigation-Oriented. The more accurate ones such as Saastamoinen, Hopfield etc (Xu, 2007) are Geodetic-oriented. They are generally more complex and require meteorological data.

In the long run, their overall accuracy is affected by the quality of the input data. The cost of quality data acquisition might be a compelling reason to resort to other models, which although less accurate, do not require any meteorological data.

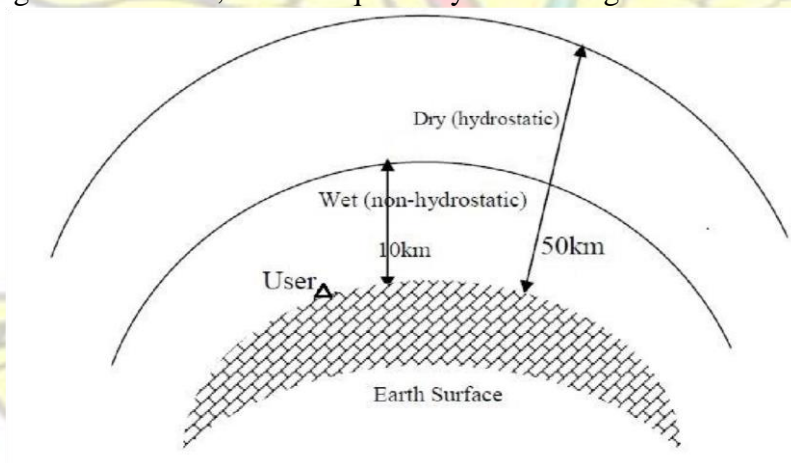


Figure 2.10: The Dry and Wet Tropospheric Components

(Dodo & Idowu, 2010)

There are models for both the wet and dry (i.e. hydrostatic) components of tropospheric delays as illustrated in Figure 2.10 above. About 90% of the tropospheric delay is attributed to the hydrostatic part alone (Hofmann-Wellenhof, et. al, 2008) which depends on surface pressure. The wet component is dependent on water vapour and

accounts for the remaining 10% of the tropospheric delay (Shrestha, 2003). It is more difficult to quantify the wet component since water vapour cannot be accurately predicted and modelled.

The following is a brief review of some of the tropospheric models used in this research.

2.6.1 THE SAASTAMOINEN MODEL

This model is based on the principle that, refractivity can be deduced from gas laws (Hofmann-Wellenhof, et. al., 2008). This is however, not without resorting to some approximations. The tropospheric delay, as modelled by Saastamoinen, is presented as follows:

$$D_z^{\text{trop}} = \frac{0.002277}{\cos z} [P + P_w \left(\frac{1255}{T} + 0.05 \right) - \tan^2 z] \dots\dots\dots(7)$$

Where z = zenith angle of satellite

P = atmospheric pressure (mbar)

T = temperature (Kelvin)

P_w = partial pressure of water vapour (mbar)

D_z^{trop} = tropospheric path delay (metres)

This model has been refined by Saastamoinen with the inclusion of two correction terms as shown in equation (8). The refined Saastamoinen model is (ibid):

$$D_z^{\text{trop}} = \frac{0.002277}{\cos z} [P + P_w \left(\frac{1255}{T} + 0.05 \right) - B \tan^2 z] + dR \dots\dots\dots(8)$$

Where B and dR are the correction terms dependent on the height of the station and the zenith angle of satellite.

All other terms are same as used in equation (7) above

2.6.2 THE HOPFIELD MODEL

This model was developed by Hopfield who used a real data with world-wide coverage, and empirically demonstrated (as follows) dry refractivity as a function of the height above the surface of the earth as (Hofmann-Wellenhof, et. al., 2008):

$$N_d^{\text{trop}}(h) = N_{d,0}^{\text{trop}} \left[\frac{h_d - h}{h_d} \right]^4 \dots\dots\dots(9)$$

Where $h_d = 40136 + 148.72 (T - 273.16)$ [m] (9b)

N_d^{trop} = dry component of the tropospheric delay
 h = height above the surface
 T = temperature (in Kelvin)

[Note that h_d is the thickness of the assumed polytropic layer]

Hopfield assumed that, both the dry and wet components of the tropospheric delay have the same functional model. Hence, the wet equivalent of equation (9) is:

$$N_w^{\text{trop}}(h) = N_{w,0}^{\text{trop}} \left[\frac{h_w - h}{h_w} \right]^4 \dots\dots\dots(10a)$$

Where the mean value used for

$$h_w = 11\,000 \text{ m} \dots\dots\dots(10b)$$

Hopfield's total tropospheric path delay is represented (in meters) in equation (11c) as the sum of both the wet component (equation 11a) and the dry component equation (11b):

$$\Delta_w^{\text{trop}}(E) = \frac{10^{-6}}{5} \frac{(-12.96T + 3.718 \times 10^5)}{\sin\sqrt{E^2 + 2.25}} \frac{e}{T} 11000 \dots\dots\dots(11a)$$

$$\Delta_w^{\text{trop}}(E) = \frac{10^{-6}}{5} \frac{77.64}{\sin\sqrt{E^2 + 6.25}} \frac{p}{T} [40\,136 + (148.72(T - 273.16))] \dots\dots(11b)$$

$$\Delta^{\text{trop}}(E) = \Delta_d^{\text{trop}}(E) + \Delta_w^{\text{trop}}(E) \dots\dots\dots(11c)$$

Where p is atmospheric pressure,

T is temperature
 e is partial pressure of water vapour and

E is the elevation angle.

2.6.3 THE GOAD-GOODMAN MODEL

The Goad and Goodman model is often referred to as the Modified Hopfield model

(Sanlioglu & Zeybek, 2012). The latter designation stems from the rewriting of

Hopfield's empirical functions by introducing lengths of position vectors instead of height above the earth's surface (Hofmann-Wellenhof, et. al., 2008) as illustrated in

Figure 2.11 below:

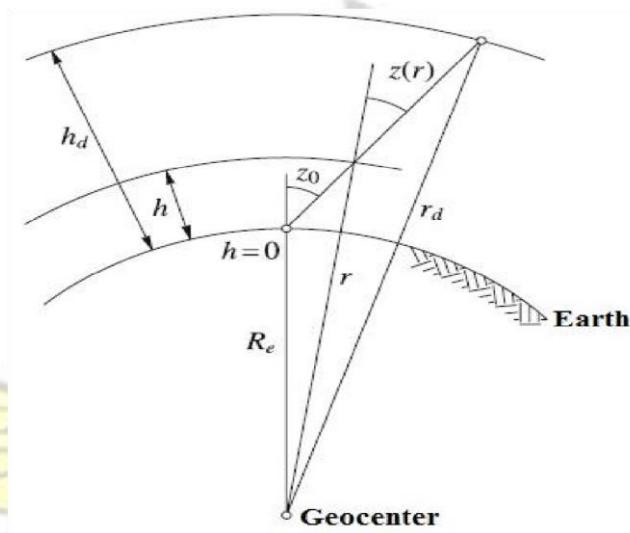


Figure 2.11: Geometry for the tropospheric path delay (ibid) Designating the radius of the earth by R_e , the corresponding lengths are

$$r_d = R_e + h_d \quad \text{and} \quad r = R_e + h$$

The refractivity for dry and wet components are given by the following expressions (Hofmann-Wellenhof, et. al., 2008) as modified versions of earlier equations (9) and (10):

$$N_d^{\text{trop}}(h) = N_{d,0}^{\text{trop}} \left[\frac{r_d - r}{r_d - R_e} \right]^4 \dots\dots\dots(12a)$$

$$N_w^{\text{trop}}(h) = N_{w,0}^{\text{trop}} \left[\frac{r_w - r}{r_w - R_e} \right]^4 \dots\dots\dots(12b)$$

Where $N_{d,0}^{\text{trop}}$ and $N_{w,0}^{\text{trop}}$ are models for the dry and wet refractivity at the

surface of the Earth

The Goad-Goodman tropospheric delay is given in equation (13) below (Hofmann-Wellenhof, et. al., 2008):

$$\Delta_i^{\text{trop}}(E) = 10^{-12} N_{i,0}^{\text{trop}} \left[\sum_{k=1}^9 \frac{\alpha_{k,i}}{k} r_i^k \right] \dots \dots \dots (13)$$

$$r_i = \sqrt{(R_e + h_i)^2 - (R_e + \cos E)^2} - R_e \sin E \dots \dots \dots (14)$$

Where

$\alpha_{1,i} = 1$	$\alpha_{6,i} = 4a_i b_i (a_i^2 + 3b_i)$
$\alpha_{2,i} = 4a_i$	$\alpha_{7,i} = b_i^2 (6a_i^2 + 4b_i)$
$\alpha_{3,i} = 6a_i^2 + 4b_i$	$\alpha_{8,i} = 4a_i b_i^3$
$\alpha_{4,i} = 4a_i (a_i^2 + 3b_i)$	$\alpha_{9,i} = b_i^4$
$\alpha_{5,i} = a_i^4 + 12a_i^2 b_i$	$=$

AND: $a_i = -\frac{\sin E}{h_i}$, $b_i = -\frac{\cos^2 E}{2h_i R_e}$

NOTE (i). The subscript i which is introduced reflects either the dry component (when replaced by d) or the wet component (when replaced by w).

(ii) E is the elevation angle. Also equal to $(90^\circ - \text{zenith})$

2.6.4 THE NIELL MODEL

The Niell Model is the result obtained from the combination of the Saastamoinen zenith path delay and the Niell mapping functions (Sanlioglu & Zeybek, 2012). It uses parameters which are calculated based on the interpolation of the average and seasonal variation (amplitude) values as functions of latitude and time.

The mapping functions for the dry and wet components of the Niell model are represented in equation (15) and (16) below (Dodo and Idowu, 2010):

$$m_d(E) = \frac{1 + \frac{a_d}{b_d}}{1 + \frac{c_d}{1 + \frac{a_d}{b_d}}} + \frac{1}{\sin E} \dots \dots \dots$$

$$\frac{\sin E + \frac{a_d}{\sin E + \frac{b_d}{\sin E + c_d}}}{\sin E + \frac{b_d}{\sin E + c_d}}$$

H

$$+ \frac{1 + \frac{a_h}{1 + \frac{b_h}{1 + c_h}}}{\sin E + \frac{a_h}{\sin E + \frac{b_h}{\sin E + c_h}}} * \frac{1}{1000} \dots\dots\dots(15)$$

$$m_w (E) = \frac{1 + \frac{a_w}{1 + \frac{b_w}{1 + c_w}}}{\sin E + \frac{a_w}{\sin E + \frac{b_w}{\sin E + c_w}}} \dots\dots\dots(16)$$

Where:

m_d and m_w are mapping functions for dry and wet components respectively.

E is satellite elevation angle

H is orthometric height a_d, b_d, c_d are coefficients in the dry component a_w, b_w, c_w are coefficients in the wet component a_h, b_h, c_h are coefficients in the height component

2.6.5 THE BLACK MODEL

The Black tropospheric model is based on the work done by Hopfield (Sanlioglu & Zeybek, 2012). The hydrostatic (B_{dry}) and wet (B_{wet}) components of the model are given below (ibid) in equations (17) and (18) respectively:

$$B_{dry} = \frac{1.552 * 10^{-5} \left[\frac{K}{hPa} \right] * \frac{p_0}{T_0} * H_d - \frac{1.92 \left[\frac{m}{o} \right]}{E^2 + 0.6^0}}{\sqrt{1 - \left(\frac{\cos E}{1 + I_c * \frac{H_d}{r}} \right)^2}} \dots\dots\dots (17)$$

$$B_{wet} = \frac{0.07465 \left[\frac{K^2}{hPa} \right] * \frac{e_0}{T_0^2} * H_T - \frac{1.92 \left[\frac{m}{o} \right]}{E^2 + 0.6^0}}{\sqrt{1 - \left(\frac{\cos E}{1 + I_c * \frac{H_T}{r}} \right)^2}} \dots\dots\dots (18)$$

Where P_o : pressure at site in [hPa]

T_o : temperature at site [K]

E: elevation angle in [degrees]

E_o : partial water vapour pressure at site in [hPa] H_d :

upper boundary height for the hydrostatic delay r:

radial distance from earth center to GPS antenna.

H_T = upper boundary height for the wet delay/height of the tropopause

$$\text{And } I_c = 0.167 - (0.076 + 0.00015 * t_o) * \exp(-0.3 \left[\frac{1}{0} \right] * E)$$

Where t_o : temperature at site in [°C]

CHAPTER THREE: METHODOLOGY AND DATA PROCESSING

As already mentioned in section 1.3, this research aims at recommending an optimum tropospheric model for baseline processing in Ghana. To achieve this aim, it was necessary to assess the performance of some standard tropospheric models using a highly precise GPS data.

For data of such quality, the researcher relied on data from the various CORS stations in the study area. This approach for the investigation of tropospheric impact was recommended by Opaluwa, et al. (2013) after conducting a similar research in Nigeria. With the CORS system, GPS signals are monitored at precisely surveyed reference sites and the data are stored for real-time or post-processing support of local geodetic surveying, mapping, geographic information systems (GIS), etc.

(Acheampong, 2008).

3.1 THE STUDY AREA

The three main stations used for this research (ie. Kumasi, Takoradi and Accra), as shown in Figures 1.1 and 1.2, constituted the only stations with permanent monuments set up during the establishment of the National CORS Network. The fourth station at

Assin-Fosu was also among the only two hub stations established as a preliminary approach to strengthen the permanent network (Poku-Gyamfi, 2009).

The network covers the Golden Triangle of Ghana which has the three largest cities in the country at the vertices. The selection of these cities was based on economic and social factors, infrastructural support, potential application and population distribution, among others. Figure 3.1 shows the study area on the map of Ghana.

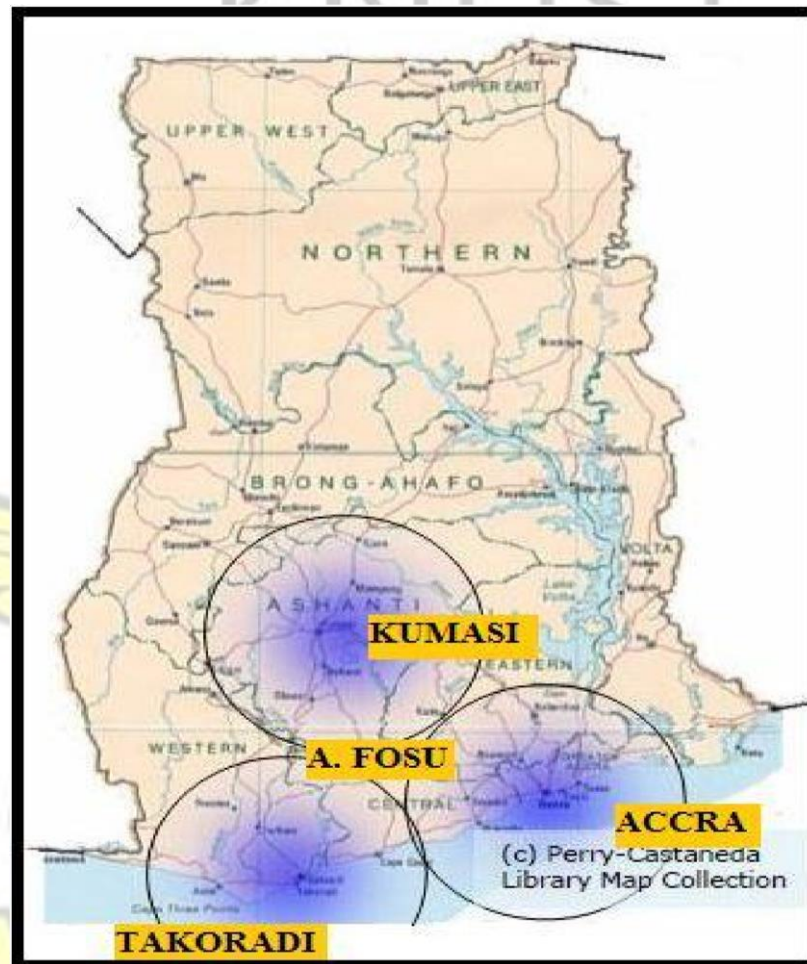


Figure 3. 1 Map showing the study area with 100km coverage of permanent Reference stations (ibid)

3.1.1 MONUMENTS

The Kumasi station is a Ground-based monument located at the premises of the Building and Road Research Institute (BRRI), of the Council for Scientific and Industrial Research of Ghana. The station is illustrated in Figure 3.2(a) and is sited about 20 meters from an office room that has been solely dedicated to the receiver and its accessories. In Accra, the monument is located on top of the Survey School Building

and is less than 10m away from the location of the receiver. The Accra station is shown below in Figure 3.2 (c). The Takoradi station (shown in Figure 3.2

(b)) is located on a rooftop and is less than 10 m from the office of the Secondi-Takoradi Regional Surveyor.



Figure 3. 2 The three permanent Monuments of Ghana CORS Network

(Courtesy: Poku-Gyamfi, 2009)

3.2 INSTRUMENTATION

The CORS, according to Fosu, et. al. (2007) primarily consists of: “A GPS Receiver, the antenna, computers, power supply and a mechanism to communicate to the outside world through broadcast of corrections to users (telemetry)”. All the above listed CORS components were employed in the data collection process except for the telemetric component. Since this research is restricted to post-processed data, there was no need for receivers that could stream data online and in real time. All data were manually downloaded periodically.

3.2.1 RECEIVER

All the receivers installed at the four stations were Sokkia GSR 2600 brand (shown in Figure 3.3). It is a dual frequency receiver and is capable of performing both RTK and post-processing applications.



Figure 3. 3 GSR2600 receiver used in data collection

Additional features include 12 L1 and 12 L2 channels as well as a removable internal Compact Flash memory card. With its power port, this receiver allows the direct use of current from the mains. However, an additional 12 V battery was connected to automatically replace the mains in the event of a power outage. It was quite robust and could endure harsh environmental conditions.

3.2.2 ANTENNA

In this research, the SOK 702 antenna type was used. This antenna utilizes the Pinwheel Technology and is shown in Figure 3.4.



Figure 3. 4 A SOK702 antenna mounted on a tripod for data collection

3.3 DATA USED

The pristine data used for this research were obtained from a 24 hour (non-stop) observations carried out concurrently on 22nd and 23rd May, 2007 at the aforementioned four stations which were all part of the National CORS network. The Long duration of observations reduces the effects of constellation of the satellites, the multipath and the troposphere delays (Acheampong, 2008). In addition, precise positioning methods such as the PPP and the DGPS (which were used in this research) required a reasonable session length so as to record quality and enough signals.

3.4 DATA PRE-PROCESSING

Using the Leica GNSS QC v2.2 software, the quality of the data was checked so as to ensure that each data passed the quality test as shown in the software report in

Table 3.1

Table 3.1 Data Quality Check Report

GENERAL TESTS	PASS /FAIL	DETAILS
Epochs with data:	Pass	Value 100.0%, Threshold 99.0 %
File Format:	Pass	
RX Clock:	Pass	
GPS SPECIFIC TESTS		
Cycle Slips:	Pass	Value 2 slips, Threshold 47 slips
Multipath:	Pass	Value 0.13m MP1 / 0.17m MP2 / 0.00m MP5, Threshold 0.5m
Data Completeness:	Pass	Value 98.3 %, Threshold 95.0%
Navigation Data:	Pass	

3.4.1 ACCURACY LIMITS FOR DGPS BASELINES

The accuracy of the data were again ascertained using two main standards by

USACE and SMD of Lands Commission, Ghana. The (USACE, 2003) specifies a

10mm plus 2ppm as minimum accuracy limit for GPS baselines of 1 to 100km. The Survey and Mapping Division (SMD, 2008) also stated, in TI 2008, a minimum limit of 10ppm for repeat baseline in any one component (x, y, z). Using these two specifications, the error limit for a 100 km baseline is computed for both standards in sections 3.4.2 and 3.4.3

3.4.2 USACE STANDARD FOR 100 KM:

$$\text{Accuracy limit for 100 km baseline} = 10\text{mm} + \frac{100 \times 1,000,000\text{mm} \times 2}{1,000,000} = 210\text{mm}$$

Hence, coordinates differences in x, y and z should not exceed 0.21 m

3.4.3 SMD STANDARD FOR 100 KM:

$$\text{Accuracy limit for 100 km baseline} = \frac{100 \times 1,000,000\text{mm} \times 10}{1,000,000} = 1000 \text{ mm}$$

Hence, coordinates differences should not exceed 1m.

The above computations were repeated for the 200km baselines and are presented in Table 3.2.

Table 3.2 Accuracy Limits for DGPS Baselines

REGULATOR	ACCURACY LIMIT	
	100km	200km
USACE	± 0.21 m	± 0.41m
SMD, (Ghana)	± 1.0 m	± 2.0 m

3.5 DATA PROCESSING

In order to work in International Terrestrial Reference Frame (ITRF) coordinates system with high accuracy, a request for online position solution of the stations was made from Natural Resources Canada (NRCan). Table 3.3 shows the resulting PPP coordinates for Assin-Fosu (FSU), Accra (ACC), Kumasi (KSI) and Takoradi (TDI) for each of the two-days.

Table 3. 3 Precise Point Positions (PPP) of Stations

DESCRIPTION	STATION	ITRF COORDINATES		
		X (m)	Y (m)	Z (m)
PPP DAY 1	FSU	6345408.107± 0.008	-141728.752 ±0.007	629324.065±0.004
PPP DAY 2	FSU	6345408.105± 0.009	-141728.751± 0.008	629324.067± 0.004
AVERA GE		6345408.106±0.009	-141728.752±0.075	629324.066±0.004
PPP DAY 1	ACC	6348052.680±0.007	-20212.884 ±0.045	617243.596±0.020
PPP DAY 2	ACC	6348052.681±0.005	-20212.882± 0.005	617243.597±0.003
AVERA GE		6348052.681±0.006	-20212.883±0.025	617243.597±0.012
PPP DAY 1	KSI	6332788.126 ±0.009	-168938.562 ±0.008	740370.541±0.001
PPP DAY 2	KSI	6332788.128± 0.009	-168938.560± 0.007	740370.540±0.004
AVERA GE		6332788.127±0.009	-168938.561±0.008	740370.541±0.003
PPP DAY 1	TDI	6352080.520±0.007	-194364.564 ±0.08	541029.388±0.003
PPP DAY 2	TDI	6352080.522±0.009	-194364.562± 0.007	541029.386± 0.004
AVERAGE		6352080.521±0.008	-194364.563±0.008	541029.387±0.004

The use of the ITRF values were to avoid any coordinate transformations which may introduce errors into the results. Also, precise point positioning (PPP) gives positions with millimeter accuracy at global scale.

3.6 TROPOSPHERIC EFFECTS ON BASELINES

Following the computation of the PPP of the various stations, a DGPS approach was adopted to use the Kumasi station as base to fix the remaining stations as rovers. A total of three baselines were processed as shown in the network diagram in Figure 3.6. After comparing the DGPS solutions with the PPP solutions, the resulting differences were used to compute the root mean square errors and the standard deviations for accuracy analysis.

The results obtained are shown in Table 4.3 and clearly meet the acceptance criteria given in Table 3.4 below by USACE for baseline distances beyond 100km.

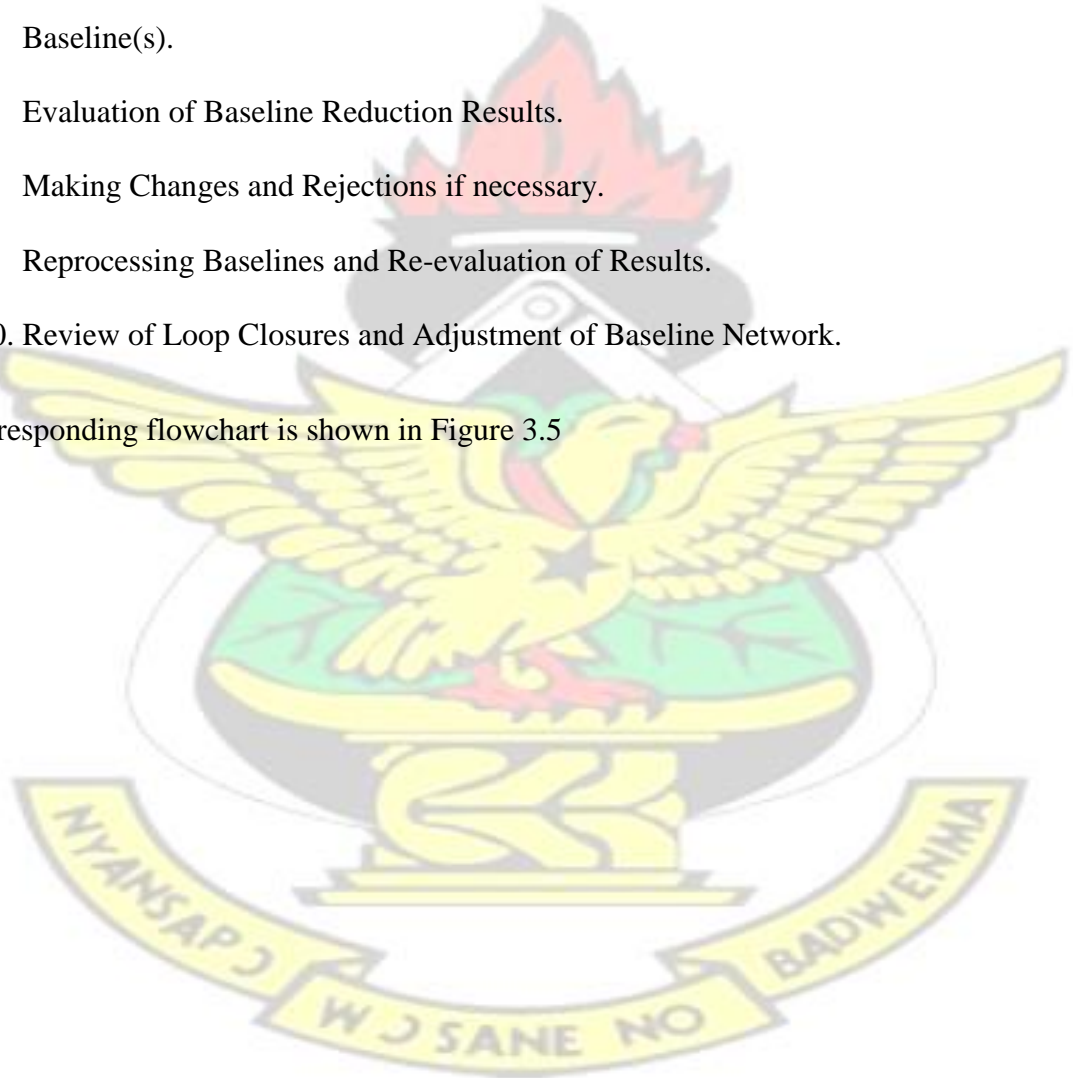
Table 3. 4 The Solution Acceptance Criteria

Distance between Receivers (km)	RMS Criteria Formulation d=distance between receivers	Formulated RMS Range (cycles)	Formulated RMS Range (meters)
0 -10	$\leq (0.02 + (0.004*d))$	0.02 – 0.06	0.004 – 0.012
10-20	$\leq (0.03 + (0.003*d))$	0.06 – 0.09	0.012 – 0.018
20-30	$\leq (0.04 + (0.0025*d))$	0.09 – 0.115	0.018 - 0.023
30-40	$\leq (0.04 + (0.0025*d)) \leq$	0.115 - 0.14	0.023 - 0.027
40-60	$(0.08 + (0.0015*d))$	0.14 - 0.17	0.027 - 0.032
60-100	≤ 0.17	0.17	0.032
> 100	≤ 0.20	0.20	0.04

The systematic processes followed in the reduction of the GPS baselines and testing of the various tropospheric models are outlined below:

1. Field observations.
2. Download/Importation of Raw GPS Data from Receivers/Data Storage Media.
3. Download Precise Ephemeris Data.
4. Pre-Processing (Edit and make changes to raw GPS Data if necessary).
5. Setting the processing style and baseline flow sequence.
6. The individual selection of various Tropospheric models and Processing of Baseline(s).
7. Evaluation of Baseline Reduction Results.
8. Making Changes and Rejections if necessary.
9. Reprocessing Baselines and Re-evaluation of Results.
10. Review of Loop Closures and Adjustment of Baseline Network.

A corresponding flowchart is shown in Figure 3.5



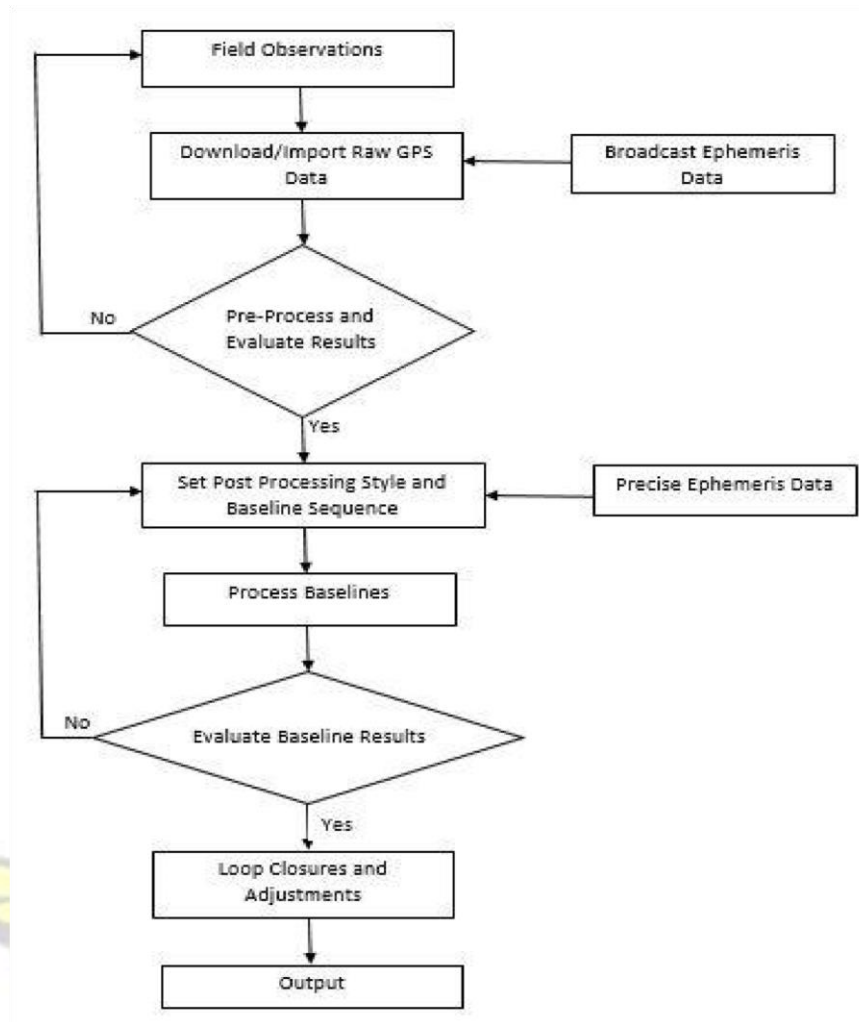


Figure 3. 5 Data Processing Routine

The pre-processing stage in the above generalized flow chart is briefly expounded as follows:

The Pre-processing consists of the conversion from patented receiver formats to RINEX, concatenation (and decimation when necessary) of RINEX files, various quality checks and RINEX smoothing. The process of smoothing and editing RINEX involves the determination and elimination of cycle slips, editing of gaps in information, checks on station names and antenna heights. In addition, a consideration of the settings of elevation mask angle is also performed during this stage.

The post-processing criterion used in the processing of the data involved the following:

- The use of the Trimble Geomatics Office (TGO) software.
- Epoch Rate of 30 seconds.
- Elevation Mask of 10 Degrees.

- L1/L2 fixed Iono-free processing style.
- Broadcast Ephemeris and Broadcast Clock Model.
- RINEX data format.
- Tropospheric model (the various tropospheric models under consideration in this study were chosen individually and the above post-processing criterion were repeated for each model).

3.7 NETWORK ADJUSTMENT

3.7.1 NETWORK PREADJUSTMENT DATA ANALYSIS

Before the adjustment of GPS networks, it is a necessary requirement that the acquired data be analyzed for internal consistency and the elimination of probable blunders (Ghilani & Wolf, 2007). To achieve this, a succession of processes must be followed. Control points are not necessarily needed in these analysis. However, based on the actual observations taken and the network geometry, the procedure may involve an analysis of the:

- Discrepancies originating from the redundancy in observing components of the baseline.
- The discrepancy in fixed and observed baseline components, and
- Loop closures.

The loop closure analysis criterion was employed in this research since the four stations in the study area formed a geometrically stable triangular network and provided sufficient checks which made it possible to perform adjustments on the points which constituted the network.

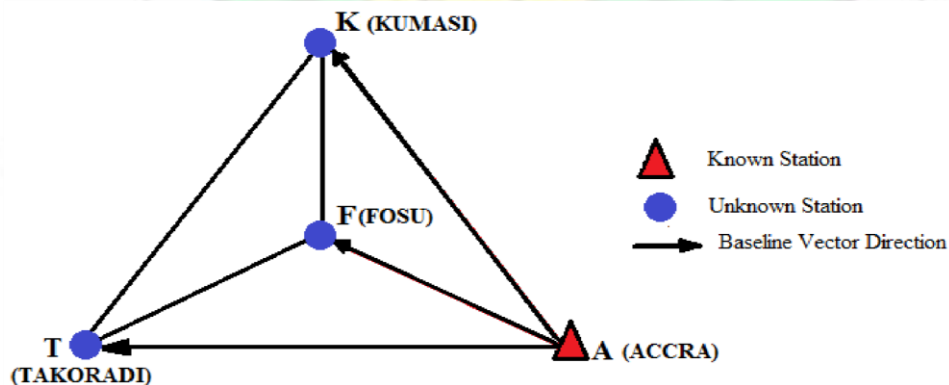


Figure 3.6 GPS Observation Network

3.7.2 LOOP CLOSURE ANALYSIS

From the GPS network shown in Figure 3.6, some closed loops could easily be noticed. For instance, a closed loop is formed by points ATFA. Others are AFKA and KFTK. For each of the closed loops, the algebraic sum of the ΔX , as well that of ΔY and ΔZ should equal zero but such perfect results are impossible to achieve in real situations.

However, any abnormally large misclosure noticed within a particular loop is an indication of either a blunder or a significant random error in either one (or even more) of the baselines of that loop.

For the computation of loop misclosures, denoted as c_x , c_y and c_z , the components of the baseline are algebraically added for that selected loop. The closures in X, Y and Z for the individual loops (in Figure 3.6 above) are:

$$\begin{aligned}
 c_{x_1} &= \Delta X_{AT} + \Delta X_{TF} + \Delta X_{FA} \\
 c_{y_1} &= \Delta Y_{AT} + \Delta Y_{TF} + \Delta Y_{FA} \dots\dots\dots \text{AFKA (Loop 1)} \\
 c_{z_1} &= \Delta Z_{AT} + \Delta Z_{TF} + \Delta Z_{FA} \\
 \\
 c_{x_2} &= \Delta X_{AF} + \Delta X_{FK} + \Delta X_{KA} \\
 c_{y_2} &= \Delta Y_{AF} + \Delta Y_{FK} + \Delta Y_{KA} \dots\dots\dots \text{ATFA (Loop 2)} \\
 c_{z_2} &= \Delta Z_{AF} + \Delta Z_{FK} + \Delta Z_{KA} \\
 c_{x_3} &= \Delta X_{KF} + \Delta X_{FT} + \Delta X_{TK} \quad c_{y_3} = \Delta Y_{KF} + \Delta Y_{FT} + \Delta Y_{TK} \\
 &\dots\dots\dots \text{KFTK (Loop 3)} \quad c_{z_3} = \Delta Z_{KF} + \Delta Z_{FT} + \Delta Z_{TK}
 \end{aligned}$$

In order to compute the resultant closure per loop, the above equations must be solved and the results used. The resultant loop closure is given by the equation (19):

$$\text{Resultant Loop Closure (ce)} = \sqrt{(c_x^2 + c_y^2 + c_z^2)} \dots\dots\dots (19)$$

For the purpose of evaluation, the expression of loop misclosures are stated in terms of the ratios of the resultant misclosures to the total loop lengths. They are given in part per million (**ppm**), calculated as:

$$\text{ppm} = \frac{ce}{\text{Loop Length}} * 1\,000\,000 \dots\dots\dots (20)$$

The resultant loop closures and the ppm of the various closed loops in the GPS observation network are presented in Table 3.5

Table 3. 5 Resultant Loop Closure -Units (m)

ΔATF				
Baseline	$\Delta X(\text{m})$	$\Delta Y(\text{m})$	$\Delta Z(\text{m})$	Distance(m)
A - T	4027.8686	-174151.619	-76214.23508	190141.0523
T - F	-6672.00942	52635.75857	88294.84777	103009.8002

F - A	2644.13584	121515.8677	-12080.61235	122143.517
Vector sum	-0.00498	0.00722	0.00034	415294.3694
Resultant closure =		0.008777494	ppm =	0.021135596
ΔAFK				
Baseline	ΔX(m)	ΔY(m)	ΔZ(m)	Distance(m)
A - F	-2644.15584	-121515.8977	12080.61235	122143.5473
F - K	-12620.38076	-27209.78601	111046.3386	115025.8048
K - A	15264.53558	148725.6876	-123126.9494	193681.6508
Vector sum	-0.00102	0.00394	0.00152	430851.0029
Resultant closure =		0.004344468	ppm =	0.010083457
ΔKFT				
Baseline	ΔX(m)	ΔY(m)	ΔZ(m)	Distance(m)
K - F	12620.38076	27209.78601	-111046.3356	115025.8019
F - T	6672.02942	-52635.75857	-88294.84077	103009.7955
T - K	-19292.40405	25425.97356	199341.1764	201880.1169
Vector sum	0.00613	0.001	0.00011	419915.7143
Resultant closure =		0.006212005	ppm =	0.014793456
ΔATK				
Baseline	ΔX(m)	ΔY(m)	ΔZ(m)	Distance(m)
A - T	4027.8686	-174151.6596	-76214.23308	190141.0886
T - K	-19292.41105	25425.97356	199341.1764	201880.1176
K - A	15264.5388	148725.6876	-123126.9494	193681.6511
Vector sum	-0.00365	0.0016	-0.00603	585702.8573
Resultant closure =		0.00722796	ppm =	0.01234066

All resultant closures ought to be below 1cm. If not, the measurements are probably inconsistent or there might be a recorded blunder in at least one of the observations. Each of the computed resultant closures satisfied this specification as can be verified in table 3.2 above. This is an indication of a high level of consistency in the data used and further indicates the absence of either blunders or random errors in any of the measured loops.

3.7.3 LEAST SQUARES ADJUSTMENT

3.7.3.1 OBSERVATION EQUATIONS

The presence of redundant observations in GPS networks requires the network to be adjusted for consistency in coordinate differences. In order to apply least squares in baseline adjustments, observation equations must be written to relate the coordinates of the stations, their observed coordinate differences as well as the residual errors. In this study, the observation equations for each measured baseline are as follows:

$$\begin{aligned}\partial_{XA} &= [X_A - X'_A] \\ \partial_{YA} &= [Y_A - Y'_A] \\ \partial_{ZA} &= [Z_A - Z'_A]\end{aligned} \quad \dots (21)$$

For baseline KA:

$$\begin{aligned}\partial_{XA} - \partial_{XK} &= [X_K + \Delta X_{KA} - X_A] \\ \partial_{YA} - \partial_{YK} &= [Y_K + \Delta Y_{KA} - Y_A] \\ \partial_{ZA} - \partial_{ZK} &= [Z_K + \Delta Z_{KA} - Z_A]\end{aligned} \quad \dots (22)$$

For baseline KT:

$$\begin{aligned}\partial_{XT} - \partial_{XK} &= [X_K + \Delta X_{KT} - X_T] \\ \partial_{YT} - \partial_{YK} &= [Y_K + \Delta Y_{KT} - Y_T] \\ \partial_{ZT} - \partial_{ZK} &= [Z_K + \Delta Z_{KT} - Z_T]\end{aligned} \quad \dots (23)$$

For baseline KF:

$$\begin{aligned}\partial_{XF} - \partial_{XK} &= [X_K + \Delta X_{KF} - X_F] \\ \partial_{YF} - \partial_{YK} &= [Y_K + \Delta Y_{KF} - Y_F] \\ \partial_{ZF} - \partial_{ZK} &= [Z_K + \Delta Z_{KF} - Z_F]\end{aligned} \quad \dots (24)$$

From Figure 4.6, a total of 6 baselines were measured, hence, the number of observation equations that can be developed is 18. Also, stations K, T and F have three unknown

coordinates each. The number of redundant observations in the network are $18 - 9 = 9$. An expression of the matrix form of the 18 observation equations is:

$$AX = L + V \dots\dots\dots (25)$$

Where

- A is the coefficient matrix (A is $m \times n$ with $m > n$)
- L is the matrix of absolute terms
- V is the residuals (errors)
- X is the matrix of unknown parameters (least-squares solution)

Using the same nomenclature above and denoting the least squares solution of unknowns by X, it can then be calculated using equation (26) below:

$$X = (A^TWA)^{-1} (A^TWL) \dots\dots\dots (26)$$

Where the Weight Matrix, $W = \text{inv}(\text{covariance matrix})$

$$\text{Reference Standard Deviation } (S_0) = \sqrt{\frac{V^T WV}{m-n}} \dots\dots\dots (27)$$

Where

- m = number of equations
- n = number of unknowns

$$(A^TWA)^{-1} = N^{-1} = Q_{ii} \dots\dots\dots (28)$$

Where

Q_{ii} is the variance-covariance matrix

$$\text{Standard Deviation of Adjusted Quantities } (S_i) = S_0 \sqrt{Q_{ii}} \dots\dots\dots (29)$$

3.8 PROCESSING SOFTWARE

Three main categories of GPS data processing software can be distinguished:

- Commercial-off-the-shelf (COTS) processing software–

This is in reference to those developed by the manufactures of the various branded GPS receivers and mostly intended to accompany their products. An example is the Trimble Geomatics Software (TGO) used in this

research (Details in section 3.8.1).

- Specialist software-

They are anticipated to be used in strictly specified applications. Some examples include data capture for Geographic Information Systems,

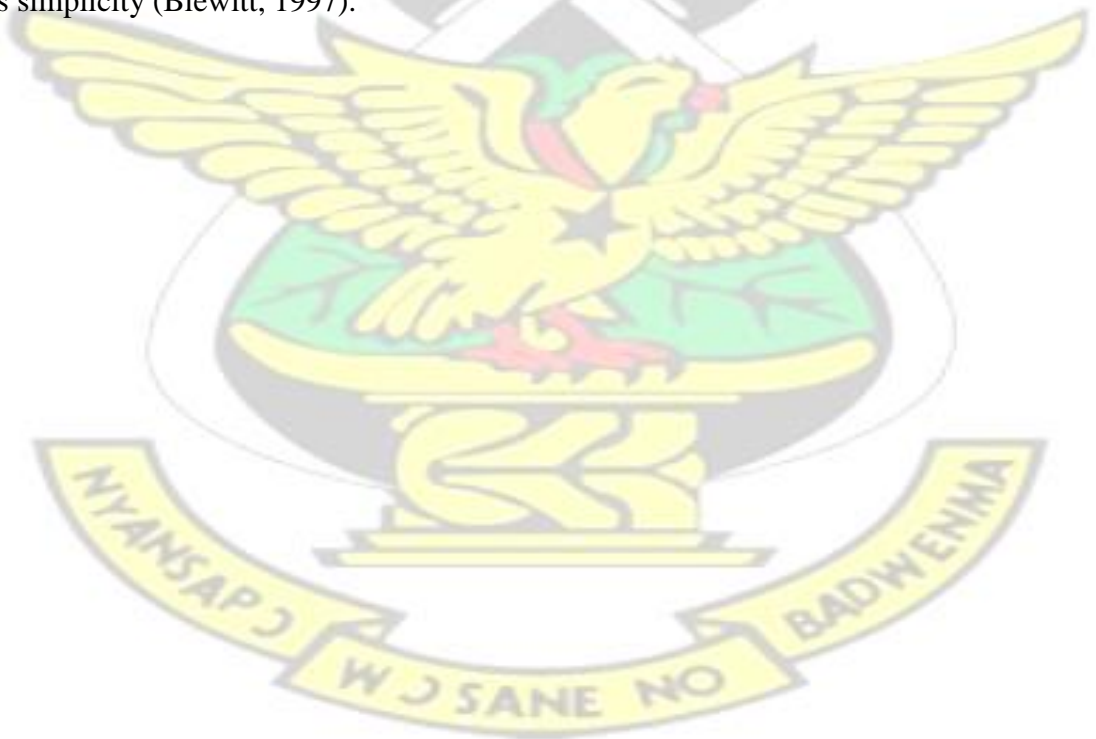
Aerial and marine related operations, determination of elevation, etc.

- Institutional/Governmental/Academic purposed software-

This group encompasses the various software designed by academic and other institutions for specific research purposes.

3.8.1 TRIMBLE GEOMATICS OFFICE (TGO)

TGO is a commercial-off-the-shelf software developed by Trimble® Navigation Limited. It is completely furnished for nearly every survey task and computes GPS vectors using Weighted Ambiguity Vector Estimator (WAVE). It uses the HTML format in the presentation of its output/results. The Trimble Geomatics Office (TGO) is a popular Commercial GNSS processing software and is one of the various Trimble products used in over 100 countries around the world (Neal, 2008). It is easy to use and does not require so much time to understand. Expert training is also not necessary due to its simplicity (Blewitt, 1997).



CHAPTER 4: RESULTS AND ANALYSIS

4.1 RESULTS

The three baselines, listed in Table 4.1, were selected for processing and the testing of the various tropospheric models using the Trimble Geomatics Office (TGO) software. The various tropospheric delay models used are

- Black,
- Goad-Goodman,
- Hopfield,
- Niell,
- Saastamoinen, and
- The case of NONE model where NO MODEL was used in the baseline processing.

Table 4. 1 Baselines and their Designations

BASELINE NAME	ABBREVIATIONS
KUMASI – ACCRA	KSI – ACC
KUMASI – ASSIN FOSU	KSI – FSU
KUMASI – TAKORADI	KSI – TDI

Table 4. 2 Tropospheric Models and their Designations

MODEL NAME	ABBREVIATIONS
BLACK	BLACK
GOAD-GOADMEN	GOGO
HOPFIELD	HOPF
NIELL	NIELL
SAASTAMOINEN	SAAST
NB: “NONE” means NO MODEL was used in the baseline processing	

According to (Chalermchon and Chalermwattanachai, 2005), “the performance of each standard tropospheric model can be characterised by the Root Mean Square Error (RMSE)”. This has been confirmed by Hamed, et. al (2013) who studied the effect of different tropospheric models and ocean tides on long baselines.

Table 4.3 below shows the resulting RMS errors following the successful systematic processing of each of the baselines versus the various tropospheric models tested whereas Figure 4.1 illustrates the RMS trend with increasing session length.

Table 4. 3 Baseline Processing Results- RMS Error per Tropospheric Model

BASELINE	BLACK (m)	GOGO (m)	HOPF (m)	NIELL (m)	SAAST (m)	NONE (m)
KSI-ACC	0.0460	0.0440	0.0430	0.0460	0.0430	0.1450
KSI-FSU	0.0240	0.0210	0.0200	0.0240	0.0200	0.1320
KSI-TDI	0.0250	0.0240	0.0230	0.0250	0.0230	0.2510
MEAN	0.0317	0.0297	0.0287	0.0317	0.0287	0.1760

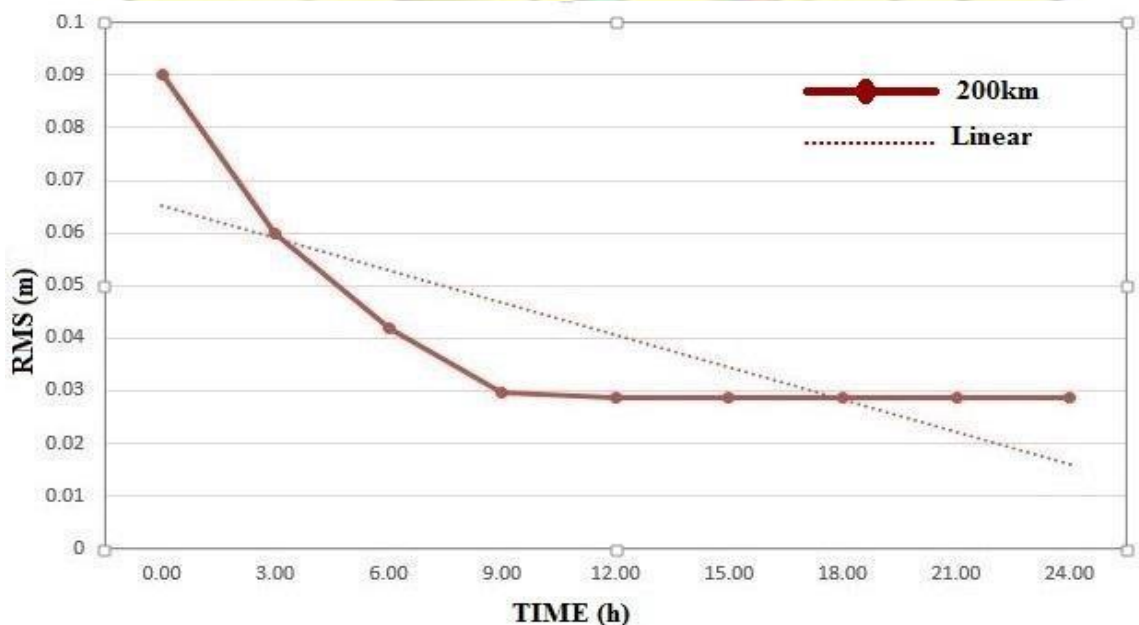


Figure 4. 1 The RMS trend with increasing observation time.

In this research, each baseline was exclusively processed by selecting a single Tropospheric model at a time. The baseline processing culminated with the “NONE” option in which no tropospheric model was incorporated in the processing procedure.

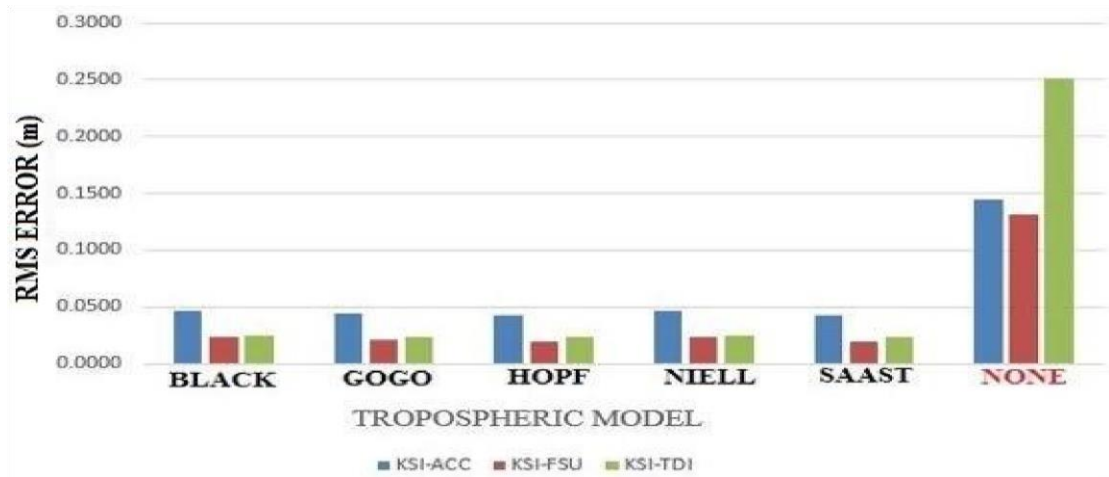


Figure 4. 2 RMS errors yielded by each Tropospheric Model

4.2 ANALYSIS

In the analysis below, the differences in the tropospheric delays yielded by each of the five tropospheric models for the various baselines are discussed.

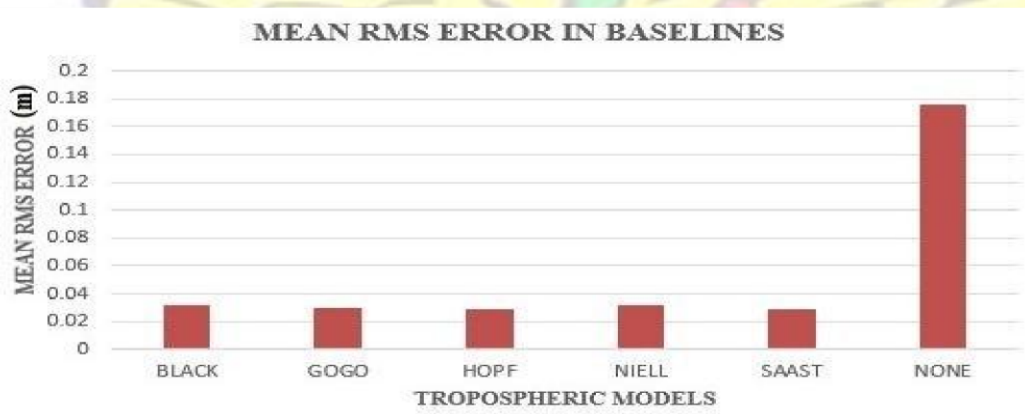


Figure 4. 3 Mean RMS error of various Tropospheric Models

For all the baselines tested, the Hopfield and Saastamoinen models consistently performed equally well and better than all the remaining models, yielding mean RMS errors of **0.0287m each**. The better performance of both the Saastamoinen and the

Hopfield models have been established in similar studies by (Chalermchon & Chalermwattanachai, 2005) in which these two Tropospheric models produced more reliable baseline results than their counterparts in the same study. Figure 4.4 illustrates the deviation of the remaining models from the top bipartite Hopfield and Saastamoinen models. It is observed that, the Goad-Goodman Model (GOGO) had the least deviation

of 0.001m, making it the next most effectual model after both Hopfield and Saastamoinen models. The third place in performance was shared as a tier between the Black and Niell models. They both deviated from the Optimum model by 0.003m each and yielded the same RMS error of 0.0317m.

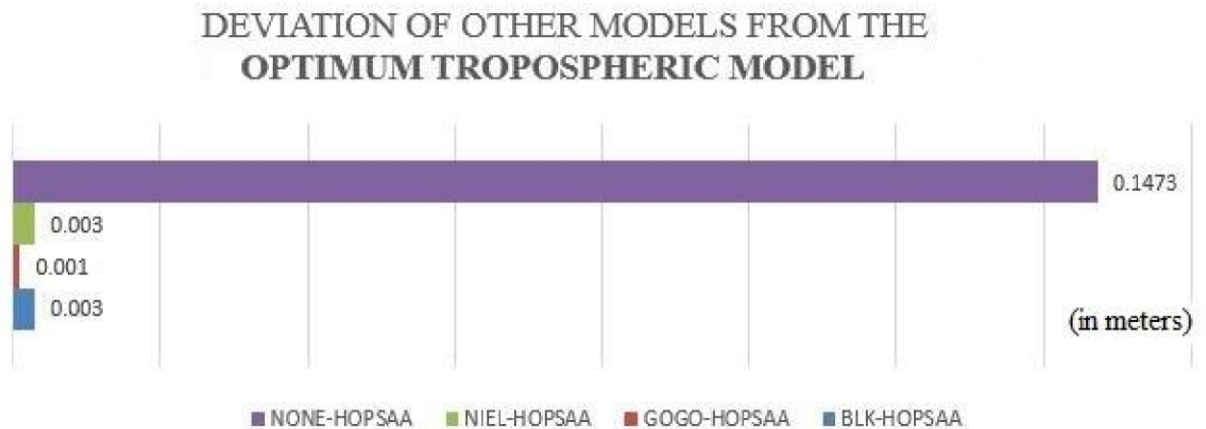


Figure 4.4 Deviation of other Models from the Optimum

The NONE model, which represents the scenario where NO TROPOSPHERIC MODEL was selected, consistently returned the worst RMS errors with a mean of **0.176m**. This represented a deviation of about 0.1473m from the Optimum Models. This is a clear indication that, processing of long baselines in Ghana, without modelling the tropospheric delays, could result in probably worse inherent errors unless higher accuracy data collection strategies (than was used in this research) are adopted. This alternative option could, however, be very expensive.

There was a consistency in the performance of all the models per baseline as illustrated in Table 4.3. That is, for all the tested Tropospheric models, the resultant RMS errors were least for the KSI-FSU baseline, followed by KSI-TDI and KSIACC baselines respectively. The only exception to this observation was in the case of the NONE model wherein the position of the KSI-TDI and KSI-ACC baselines were interchanged.

However, in relation to the length of baselines and the performance of the tropospheric models, no correlation was incontrovertibly established. This is illustrated in Figure 4.5 below which juxtaposes both the RMS errors and the length of baselines.

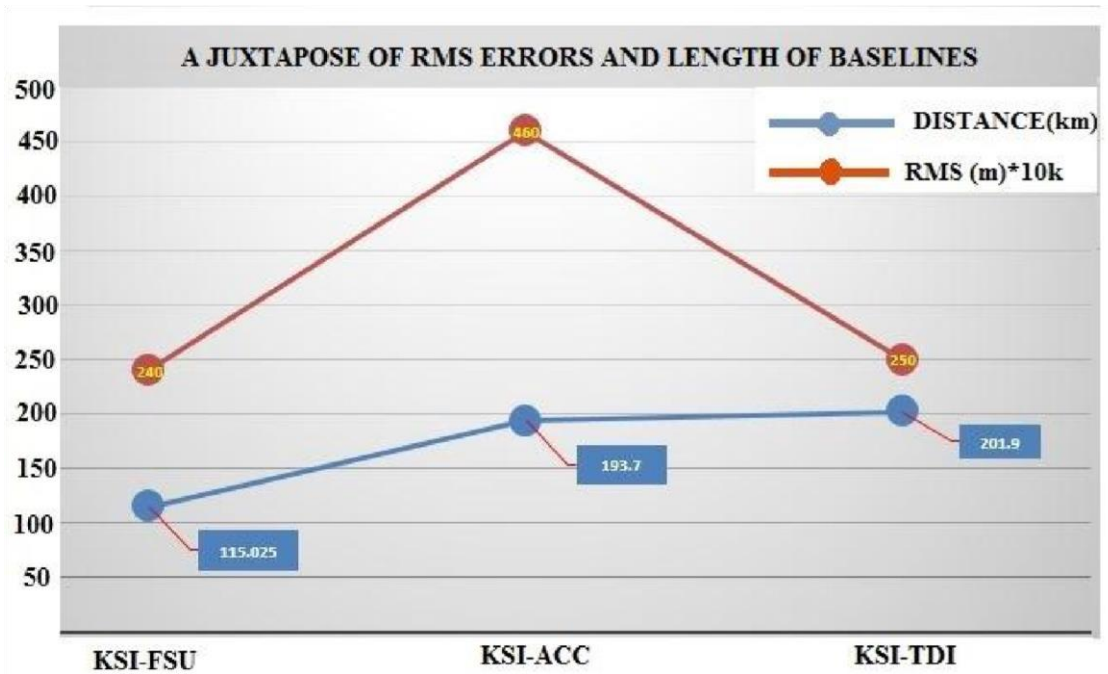


Figure 4. 5 Juxtaposing RMS and Length of Baselines

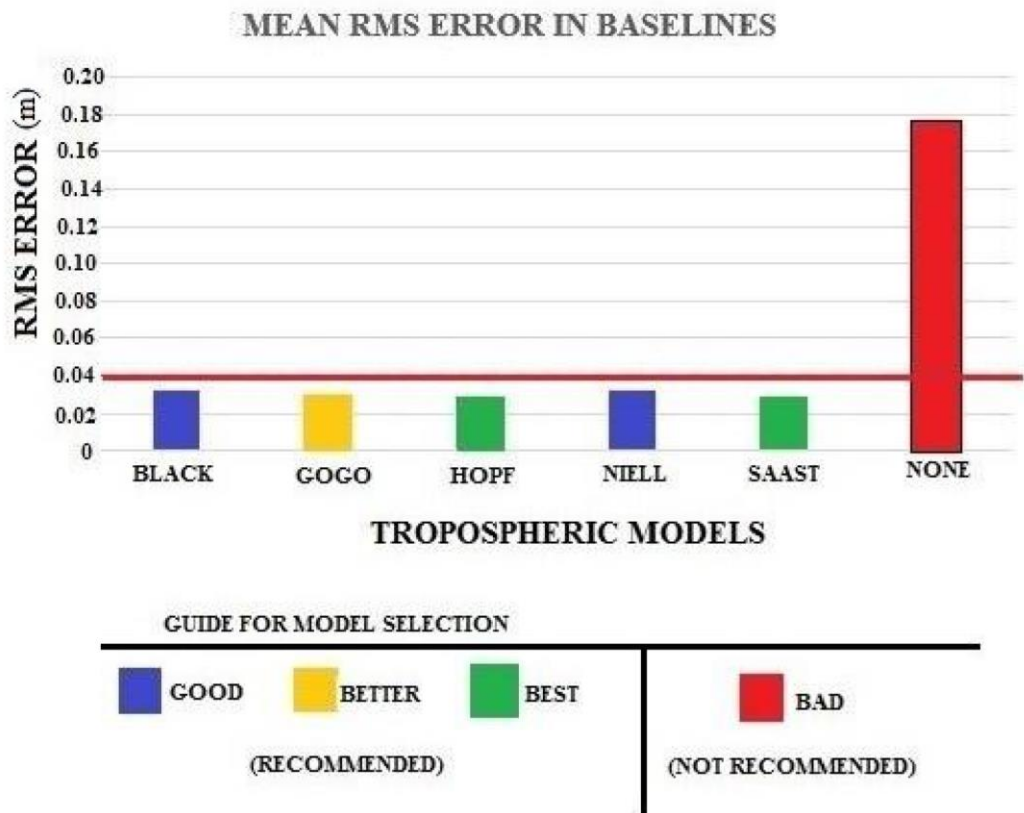


Figure 4. 6 All models passed except for the NONE instance

CHAPTER 5: CONCLUSION AND RECOMMENDATION

5.1 CONCLUSION

This study commenced with the objective to estimate, using TGO, the amount of tropospheric delay yielded by the five selected tropospheric models. Afterwards, the selected baselines were processed without modelling the tropospheric delays. The differences in the estimated tropospheric delays were also examined in order to achieve the ultimate aim of recommending the optimum tropospheric model for baseline processing in Ghana.

The results from the set objectives have been represented both quantitatively and graphically. Analysis made on these quantities and graphs has demonstrated the performance of the Saastamoinen, Hopfield, Goad-Goodman, Niell and Black

models on the processing of baselines. It has also elucidated the effect of ignoring the tropospheric component in baseline processing. In consideration of the findings and the analysis performed, all the aforementioned objectives have been achieved and the following conclusions have been drawn.

- **Each of the tropospheric models passed the accuracy criteria**

Based on the findings from this study, with particular references to Figure 4.3 and table 4.3, it can be concluded that the accuracy of each tested tropospheric model cannot be disputed. From the least RMS of 0.0287m of Hopfield and Saastamoinen, through the 0.0297m of Goad-Goodman to the highest 0.0317m of Black and Niell models, all the RMS values passed the USACE criteria of 0.04m for baselines beyond 100km.

- **Processing baselines without tropospheric models produces unacceptable results:** In the “NONE” instance where tropospheric models were ignored in the processing of the

various baselines, the results was an outrageous mean RMS error of 0.176m. As shown in figure 4.6, it is more than three times greater than the 0.04m accuracy limit. Even in the case of KSI-TDI baseline (from table 4.3), the RMS error was 0.211m more incorrect. It is therefore concluded that, baselines processed without a model for correcting tropospheric delays would be incorrect for high precision surveys. Surveyors must therefore avoid processing baselines without tropospheric models. Apart from the optimum model recommended below, the choice of any other tropospheric model may be at least better than none at all as illustrated in

Figure 4.6.

- **The optimum tropospheric models are the Hopfield and the**

Saastamoinen models. The Figure 4.6, is a graphical representation of all the models studied and their performance based on the USACE accuracy specifications. All models whose mean RMS error fell below the accuracy limit of 0.04m are recommended but rated to be GOOD, BETTER and BEST. The Hopfield and Saastamoinen (HOPF & SAAST) models both had the most accurate RMS error of 0.0287m achieved in the study. The deviation of the other models from this is illustrated by figure 4.4. In conclusion, any of the five models examined this research performed well in the study area. Nevertheless, the choice of either the Hopfield or the Saastamoinen models is optimum for the processing of baselines in Ghana.

5.2 RECOMMENDATIONS

The researcher would like to make the following recommendations based on the findings and observations from this study:

1. A similar research must be carried out in the Northern sector of Ghana to establish whether the climactic disparity in the Northern and Southern sectors have any impact on the performance of tropospheric models in Ghana.
2. Due to their affordability and popularity among surveyors in Ghana, it is recommended that Single frequency receivers be used to conduct a similar research for a comparative analysis with the findings from this work.

KNUST

REFERENCES

- Acheampong, A. A. (2008, June). Developing a differential GPS (DGPS) Service in Ghana. An MPhil Dissertation. Department of Geomatic Engineering, Kumasi, Ghana. Retrieved June 3, 2015, from <http://ir.knust.edu.gh/bitstream/123456789/667/1/Thesis.pdf>
- Almanac, T. (2015, January). Retrieved May 27, 2015, from GPS World website: http://gpsworld.com/wpcontent/uploads/2015/01/GPS_World_Almanac_Jan2015.pdf
- Arbesser-Rastburg, B. (2002). Ionospheric and Tropospheric Modelling and Monitoring for GNSS at the European Space Agency. Noordwijk, Netherlands: International Union of Radio Science. Retrieved June 3, 2015, from <http://www.ursi.org/proceedings/procGA11/ursi/FG-1.pdf>
- BDS. (2015, May 26). System Introduction: Service Target. Retrieved from BeiDou Navigation Satellite System: <http://www.beidou.gov.cn>
- Bidikar, B., Rao, G. S., Ganesh, L., & Kumar, M. S. (2014). "Satellite Clock Error and Orbital Solution Error Estimation for Precise Navigation Applications," Positioning, Vol. 5(No. 1), pp. 22-26. doi:10.4236/pos.2014.51003.
- Blewitt, G. (1997). Geodetic Applications of GPS. Swedish Land Survey.
- Cavcar, M. (2014, April 6). The International Standard Atmosphere. Retrieved June 5, 2015, from ANADOLU ÜNİVERSİTESİ - KİŞİSEL WEB SAYFALARI:

- <http://home.anadolu.edu.tr/~mcavcar/common/ISAweb.pdf>
Chalermchon, S., & Chalermwattanachai, P. (2005). Impact of Different Tropospheric Models on GPS Baseline Accuracy: A Case Study in Thailand. *Journal of Global Positioning Systems*, Vol. 4, No. 1-2: 36-40.
- Conley, R., Cosentino, R., Hegarty, C. J., Kaplan, E. D., Leva, J. L., Haag, M. U., & Dyke, K. V. (2006). Performance of Stand-Alone GPS. In *Understanding GPS: Principles and Applications* (pp. 304-305). Norwood: ARTECH HOUSE, INC.
- CSNO. (2013). Report on the Development of BeiDou Navigation Satellite System (Version 2.2). China Satellite Navigation Office. doi:<http://www.beidou.gov.cn/attach/2013/12/26/20131226fed336adf2184d52843d5bf81832e82c.pdf>
- Dana, P. H. (2015, February 2). Global Positioning System Overview. (T. U. Department of Geography, Producer) Retrieved from http://www.colorado.edu/geography/gcraft/notes/gps/gps_f.html
- Dodo, J. D., & Idowu, T. O. (2010). Regional Assessment of the GPS Tropospheric Delay Models on the African GNSS Network. *Journal of Emerging Trends in Engineering and Applied Sciences (JETEAS)* 1 (1), 113-121. Retrieved from jeteas.scholarlinkresearch.org
- EGNOS. (2015). About EGNOS: What is SBAS? Retrieved May 27, 2015, from EGNOS website: <http://egnos-portal.gsa.europa.eu/discover-egnos/about-egnos/what-sbas>
- El-Arini, M. B. (2008). Tropospheric Effects on GNSS. Santiago, Chile: The MITRE Corporation. Retrieved June 4, 2015, from <http://www.icao.int/SAM/Documents/2008/IONOSFERASEMINAR/Tropospheric%20Effect%20on%20GNSS.pdf>
- ESA. (2015, May 24). Retrieved from European Space Navigation: http://www.esa.int/Our_Activities/Navigation/The_future_-_Galileo/What_is_Galileo
- FIG. (2013). News: News 2013. Retrieved May 26, 2015, from International Federation of Surveyors: http://fig.net/news/news_2013/fig2013/index.asp
- Fosu. (Personal Communication, 2015, July 23). Head of Department, Geomatic

Engineering, KNUST.

Fosu, C., Poku-Gyamfi, Y., & Hein, G. W. (2007, August). Global Navigation Satellite System (GNSS) – A Utility for Sustainable Development in Ghana. *Journal of Science and Technology*, 27(2), 130-138.

Ghilani, C. D., & Wolf, P. R. (2007). *Elementary Surveying - An Introduction to Geomatics*. New Jersey: Pearson Prentice Hall.

GLONASS. (2015). Constellation Status. , 2015. <https://glonass-iac.ru/en/> GLONASS/ Date Retrieved: May 20th, 2015 .

GPS.gov. (2015, February 2). Retrieved from GPS.gov: <http://www.gps.gov/policy/funding/#privatize>

GPS.gov. (2015, January 31). Systems:Control Segment. Retrieved from Official US Government website for GPS: <http://www.gps.gov/systems/gps/control/>

Griego, N. (. (2015, February 18). GPS navigates heritage celebration. Retrieved from Schriever Air Force Base website: <http://www.schriever.af.mil/news/story.asp?id=123438097>

GSC. (2015, May 24). FAQs. Retrieved from European GNSS Service Centre: <http://www.gsc-europa.eu/helpdesk/faqs>

Guochang, X. D.-I. (2007). *GPS Theory, Algorithms and Applications*. Springer-Verlag Berlin Heidelberg.

Hamed, M., Shaker, A., Saad, A., & Mahmoud, S. (n.d.). *The Effect of Different Tropospheric Models and Ocean Tide on long Baselines*.

Heather, H., & Christine, J. (2011, June 24). *AFENET MANUAL FOR TRAINEES*.

African Field Epidemiology Network (AFENET) Public Health Participatory Epidemiology Introductory Training Module, V1. Nairobi, Kenya. Retrieved June 2, 2015, from <https://cgspace.cgiar.org/bitstream/handle/10568/24715/onehealthmanual.pdf?sequence=1>

- Hofmann-Wellenhof, B., Lichtenegger, H., & Wasle, E. (2008). GNSS – Global Navigation Satellite Systems (GPS, GLONASS, Galileo and More). New York: Springer-Verlag Wien.
- Hugentobler, U., Schaer, S., & Fridez, P. (2001). Bernese GPS software, Version 4.2., Astronomical Institute, University of Bern, Switzerland.
- ICG. (2007, December). ICG (A forum to discuss Global Navigation Satellite Systems (GNSS)). Austria: Secretariat of the International Committee on Global Navigation Satellite Systems United Nations Office for Outer Space Affairs. doi:http://www.unoosa.org/pdf/publications/icg_book01E.pdf
- Jensen, A. B. (2000). Real Time Modelling of the Troposphere for Network RTK. NKG Satellite Geodesy WG Meeting at Onsala Space Observatory.
- Kaplan, E. D., & Hegarty, C. J. (2006). Understanding GPS Principles and Applications. Norwood: Artech House, INC.
- Kleijer, F. (2004). Troposphere Modeling and Filtering for Precise GPS Leveling. PhD Dissertation, Mathematical Geodesy and Positioning, Faculty of Aerospace Engineering, Delft University of Technology, the Netherlands.
- Kumar, M. (2014). GNSS Reflectometry: Making use of Multipath for altimeter measurements! Retrieved June 3, 2015, from <http://geoawesomeness.com/gnss-reflectometry-making-use-multipath-altimeter-measurements/>
- McDonald, K. D. (2002). The Modernization of GPS: Plans, New Capabilities and the Future Relationship to Galileo. *Journal of Global Positioning Systems* (2002) Vol. 1, No. 1: 1-17. Retrieved from <http://www.scirp.org/journal/PaperDownload.aspx?paperID=199>
- Mendes, V. B. (1999). Modelling the Neutral-Atmospheric Propagation Delay in Radiometric Space Techniques. PhD Dissertation, University of New Brunswick, Fredericton, Canada.
- Neal, J. (2008, June 24). Trimble Navigation Continues to Gain Market Share. Retrieved April 22, 2015, from www.forbes.com/feeds/options/2008/06/24/options19734.html
- NIGCOMSAT. (2015, May 26). Home: Who We Are. Retrieved from Nigerian Communications Satellite Website: <http://nigcomsat.gov.ng/index.php>

- Opaluwa, Y. D., Adejare, Q. A., Suleyman, Z. A., Abazu, I. C., Adewale, T. O., Odesanmi, A., & Okorochoa, V. (2013). Comparative Analysis of Five Standard Dry Tropospheric Delay Models for Estimation of Dry Tropospheric Delay in Gns Positioning. *American Journal of Geographic Information System*, 121-131. doi:10.5923/j.ajgis.20130204.05
- Poku-Gyamfi, Y. (2009, 11 16). ESTABLISHMENT OF GPS REFERENCE NETWORK IN GHANA, PhD Dissertation. Universität der Bundeswehr München.
- Rasher, M. (2009). Optimizing PNT for Agriculture and Natural Resources. CGSIC USSLS Regional Meeting, June 23-24, Honolulu, Hawaii. <http://www.gps.gov/cgsic/states/2009/honolulu/rasher.pdf>.
- Rizos, C. (1997). Principles and Practice of GPS Surveying. Monograph 17, School of Geomatic Engineering, The University of New South Wales, 555pp.
- ROB. (2012, February 09). Introduction. TROPOSPHERIC DELAY AND GNSS SIGNALS: TUTORIAL . Royal Observatory of Belgium. Retrieved June 4, 2015, from Royal Observatory of Belgium : http://gnss.be/troposphere_tutorial.php
- Ryan, S. J. (2002). Augmentation of DGPS for Marine Navigation. University of Calgary, Department of Geomatics Engineering. Alberta: UCGE Reports Number 20164. Retrieved May 27, 2015, from http://www.ucalgary.ca/engo_webdocs/GL/02.20164.SJRyan.pdf
- Saastamoinen, J. (1972). Atmospheric correction for troposphere and stratosphere in radio ranging of satellites. *Geophysical monograph*, 15, American Geophysical Union, (pp. 247-252). Washington, D.C.
- Sahmoudi, M., & Landry, R. J. (2008). Multipath Mitigation Techniques Using Maximum-Likelihood Principle. *InsideGNSS*(November / December), 24. Retrieved June 3, 2015, from <http://www.jpier.org/PIERM/pierm21/10.11080811.pdf>
- Sanlioglu, İ., & Zeybek, M. (2012, May 6-10). Investigation on GPS Heighting Accuracy with Use of Tropospheric Models in Commercial GPS Software for Different Heights. Knowing to manage the territory, protect the environment, evaluate the cultural heritage. Rome, Italy: FIG Working Week 2012.
- Schofield, W., & Breach, M. (2007). *Engineering Surveying* (6th Edition ed.).

Oxford: Elsevier Ltd.

Shaba, H. A. (2012). Nigerian Space Program and African Regional Perspectives.

Retrieved May 26, 2015, from <http://www.unoosa.org/pdf/pres/stsc2012/2012ind-03E.pdf>

Shrestha, S. M. (2003, July). Investigations into the Estimation of Tropospheric

Delay and Wet Refractivity Using GPS Measurements. UCGE Reports

(20180). Retrieved from <http://www.geomatics.ucalgary.ca/links/GradTheses.html>

Shytermeja, E. (2013). Innovative GNSS Interference Mitigation Technique. United

Nations/Croatia Workshop on the Applications of Global Navigation Satellite Systems. 21 – 25 April, pp. 6-7. Croatia: www.unoosa.org. Retrieved June 3, 2015, from <http://www.unoosa.org/pdf/sap/2013/croatia/1.3.pdf>

SMD. (2008). Technical Instructions for Spatial Data Collection and Presentation in

Ghana. Survey and Mapping Division of Ghana.

Stanford-Solar-Center. (2015, June 4). The Earth's Ionosphere. Retrieved from Stanford solar Center Web site: <http://solar-center.stanford.edu/SID/activities/ionosphere.html>

Stone, P. (2015, January 29). DoD News: News Article. Retrieved from US Department of Defense Web site: <http://www.defense.gov/news/newsarticle.aspx?id=42805>

Talay, T. A. (1975). Introduction to the Aerodynamics of Flight, NASA SP-367,. 69. Retrieved June 5, 2015, from <http://history.nasa.gov/SP-367/chapt2.htm#2a>

Thinglink. (2016). Layers in the atmosphere. thinglink.com. Retrieved April 27, 2016, from <https://www.thinglink.com/scene/633011427589750785>

Tuka, A., & El-Mowafy, A. (2012). Performance evaluation of different troposphere delay models and mapping functions. Department of Spatial Sciences, Curtin University, Australia. Retrieved February 17th, 2015, from <http://www.sciencedirect.com/science/article/pii/S0263224112003879>

Turner, D. A. (2015). GPS Civil Service Update & U.S. International GNSS Activities. China Satellite Navigation Conference 2015 (p. 7). Xi'an,: GPS.gov. Retrieved May 18, 2015, from <http://www.gps.gov/multimedia/presentations/2015/05/CSNC/turner.pdf>

USACE. (2003, July 1). NAVSTAR Global Positioning System Surveying. Washington: US Army Corps of Engineers.

Warnant, R. (2002). ATMOSPHERIC PERTURBATIONS ON GNSS SIGNALS AND THEIR INFLUENCE ON TIME TRANSFER. XXVII th General

Assembly. Maastricht: International Union of Radio Science. Retrieved June

3, 2015, from <http://www.ursi.org/Proceedings/ProcGA02/papers/p0572.pdf>

Wooden, W. (1985). Navstar Global Positioning System. Proceedings of the first International Symposium on Precise Positioning with Global Positioning System. Rockville, Maryland, April 15-19, vol. 1, pp 23-32. .

Xu, G. (2007). GPS Theory, Algorithms and Applications. Springer-Verlag Berlin

Heidelberg.

Yang, Y. (2006, May 14). Aerodynamics Handout (chapter 3) . Retrieved June 5,

2015, from Western Michigan University website: <http://homepages.wmich.edu/~y3yang/files/handouts/stanATMhandout.pdf>

Yedukondalu, K., Sarma, A. D., & Srinivas, V. S. (2011). Estimation and Mitigation of gps Multipath Interference using Adaptive Filtering. Progress In Electromagnetics Research , 21(M), 133–148. Retrieved June 3, 2015, from <http://www.jpier.org/PIERM/pierm21/10.11080811.pdf>

Zheng, Y. (2006, August). Generation of Network-Based Differential Corrections for Regional GNSS Services. A PhD Dissertation, 45-46. Australia: Queensland University of Technology. Retrieved June 3, 2015, from http://eprints.qut.edu.au/16359/1/Yi_Zheng_Thesis.pdf